



# Effect of dispersing single and hybrid nanoparticles on tribological, thermo-physical, and stability characteristics of lubricants: a review

C. Pownraj<sup>1</sup> · A. Valan Arasu<sup>1</sup>

Received: 25 March 2020 / Accepted: 13 May 2020 / Published online: 30 May 2020  
© Akadémiai Kiadó, Budapest, Hungary 2020

## Abstract

Lubricants are widely used in various mechanical systems for reducing heat and friction between the working components having relative motions. Thus, the enhancement of lubricant oil properties will play a vital role in the context of protecting machinery from highly probable damages and minimizing energy losses. The development of modern lubricants and their proper use are of great importance for managing economy and the environment. In general, nano-sized particles dispersed in the lubricants, known as nanolubricants, are used in mechanical systems in order to reduce heat and friction effectively. Properties (tribological and thermo-physical) of nanolubricants are found to be the recent subject of research in the field of lubricants. This review article comprehensively analyzes and summarizes the numerous research works on preparation, tribological property, thermo-physical property, and stability characteristics of both mono- and hybrid nanoparticle-based nanolubricants. More importantly, this paper examines the various influencing factors like base lubricants, nanoparticle size, shape, preparation methods, concentrations, nature of nanoparticles, surfactants, and temperature on nanolubricant characteristics. Finally, stability of nanolubricant, various surfactants used and different stability measuring techniques are analyzed.

**Keywords** Nanolubricants · Preparation · Tribological properties · Thermo-physical properties · Stability

## Acronyms

AES	Auger electron spectroscopy	DTC8	Dithiocarbamate
AFM	Atomic force microscopy	DLVO	Derjaguin, Landau, Verwey, and Overbeek
ASTM	American Society for Testing and Materials	EELS	Electron energy loss spectroscopy
A 336	Methoxy-tricaprylamine chloride	EDX/EDAX/EDS	Energy-dispersive X-ray spectroscopy
BNNP	Boron nitride nanoparticles	EG	Ethylene glycol
CeF <sub>3</sub>	Cerium tri-fluoride	FESEM	Field emission scanning electron microscopy
CeO <sub>2</sub>	Cerium oxide	FTIR	Fourier transform infrared spectroscopy
COF	Co-efficient of friction ( $\mu$ )	GNS	Graphene nanosheets
CNCs	Cellulose nano-crystals	H-BN	Hexagonal-boron nitride
CNBs	Carbon nano-balls	HNTs	Halloysite clay nanotubes
CNHs	Carbon nano-horns	HRTEM	High-resolution transmission electron microscopy
CTAB	Cetyltrimethylammonium bromide	HLB	Hydrophilic–lipophilic balance
C <sub>60</sub>	Fullerene	IF-MoS <sub>2</sub>	Inorganic fullerene-like molybdenum disulfide
DDSA	Dodecyl succinic anhydride	KH-560	3-Glycidoxy propyl trimethoxysilane
DLS	Dynamic light scattering	mV	Milli volt
		MWCNTs	Multi-walled carbon nanotubes
		N	Newton
		OA	Oleic acid
		OM	Optical microscope

✉ A. Valan Arasu  
avamech@tce.edu

C. Pownraj  
pownnanomech@gmail.com

<sup>1</sup> Department of Mechanical Engineering, Thiagarajar College of Engineering, Madurai, Tamilnadu 625015, India

PAG	Poly-alkylene-glycol
PAO	Poly-alpha-olefin
rGo	Reduced graphene oxide
SAE	Society of Automotive Engineers
SDS	Sodium dodecyl sulfate
SDBS	Sodium dodecylbenzenesulfonate
SEM	Scanning electron microscopy
SWCNTs	Single-walled carbon nanotubes
Span 80	Sorbitanmonooleate
TEM	Transmission electron microscopy
Tween 20	Polysorbate 20
Tween 80	Polysorbate 80
T-101	Calcium alkyl sulfonate
T-154	Polysobutene-butenediimide
UV	Ultra-violet spectroscopy
WS <sub>2</sub>	Tungsten sulfate
XPS	X-ray photoelectron spectroscopy
XRD	X-ray diffraction

## Introduction

The roots of lubricants are biological and non-biological, providing a huge number of hydrocarbon compounds. Recent technological advancements place a severe and diversified demands on lubricants. The selection and formulation of corresponding mixtures of hydrocarbons for lubrication becomes a very complex process and requires skill. Most natural oils contain substances which can hinder their lubrication properties, despite containing compounds essential for the lubrication process. Natural oils or mineral oil-based lubricants are partly refined and partly impure. An appropriate balance between impurity and purity is crucial to the oil's oxidation stability, and it differs depending on the application of the selected lubricant. Plain mineral oil, 95% and additives, 5% is the general composition of a conventional lubricating oil. The physical properties of oil depend on its base stock [1–3]. There are three sources of oils available in the market (Fig. 1). The oils manufactured from these three sources namely biological, mineral, and synthetic show different properties and are suitable for various applications. For example, biological oils are used where the risk of contamination is to be minimized, i.e., in the food and pharmaceutical industry.

They are mainly used in lubricate kilns, bakery, oven, etc. There are primarily two sources of this type of oil: vegetable and animal oil. Caster, palm, and rape-seed oils are few examples of vegetable oils, while the examples of animal oils are sperm, fish, and wool oils and sheep (lanolin). Synthetic oils are artificial substitutes for mineral oils and are specifically developed to provide lubricants with superior properties to mineral oils. For instance, temperature resistant synthetic oils being used in high-performance machinery

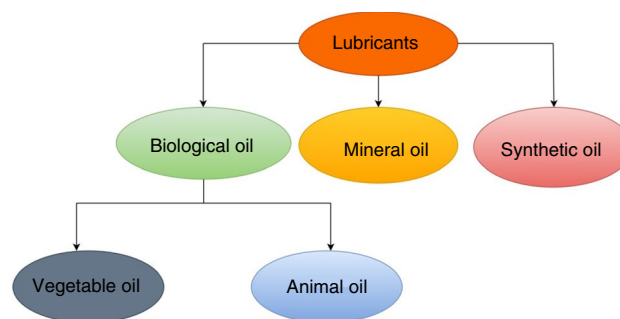


Fig. 1 Types of oils

operating at high temperature. Synthetic oils are also available for very low-temperature applications. Mineral oils, petroleum-based, are the most commonly used lubricants throughout the industry and in places where temperature requirements are reasonable. Typical applications of mineral oils are to gears, bearings, engines, turbines, etc. [2, 3].

Most of the energy losses occur due to heat and friction within the machine system. The energy loss due to heat and friction in all over the world is estimated to be about 30–50%, which is the most significant expenditure of energy in the world. On a closer look, the friction loss in an internal combustion engine, between piston ring and cylinder liner interface (about 40–50%), can be minimized effectively by using nanolubricants. The cost of machinery spare parts is estimated to be about 5% of GDP (gross domestic product) per annum. Lubricants play a vital role in increasing the lifespan of a machine (VTT Research report 2016). According to the 2014–2020 censuses, the demand for lubricants is expected to reach 44,165.11 kilo tones by the end of 2020 globally (Transparency market research). Thus, there is a paramount need to develop high-quality lubricants possessing excellent tribological and thermal properties to ensure the stability and safety of the machineries [1–10].

In recent times, nanoparticles are added into the lubricating oil to enhance its tribological and thermo-physical properties. Nanolubricants can reduce friction up to 80% than base lubricating oil. A research report states that 100 million oil barrels per year can be saved, if nanolubricants are used [1, 2, 9]. Over the past decades, the nano-particles used by researchers are: (1) metallic nano-particles; Ag [4], Cu/Zn [5], WS<sub>2</sub> [6], Bi [7], (2) metal oxide nano-particles; Al<sub>2</sub>O<sub>3</sub> [8, 9, 11–15], CuO [10, 13, 16–26], ZnO [8, 25, 26], ZrO<sub>2</sub> [28], SiO<sub>2</sub> [12, 14, 23, 29–31], Fe<sub>2</sub>O<sub>4</sub> [32–34], MgO [35], (3) carbon nanoparticles; fullerene [23, 36–38], graphene [36–40], SWCNH's [41], MWCNT's [36, 42, 43], carbon nano-ball [36], nano-diamond [31, 44] and graphite [45–47], (4) composite nanoparticles Cu–Zn [5], Ag–MoS<sub>2</sub> [4], Bi–Cu [7], Al<sub>2</sub>O<sub>3</sub>–SiO<sub>2</sub> [12], Al<sub>2</sub>O<sub>3</sub>–TiO<sub>2</sub> [15], TiO<sub>2</sub>–SiO<sub>2</sub> [30], CuO–ZnO [43], Mn<sub>0.78</sub>Zn<sub>0.22</sub>Fe<sub>2</sub>O<sub>3</sub> [33], graphene-copper [21, 48], rhenium-doped fullerene–MoS<sub>2</sub> [49], IF–MoS<sub>2</sub>

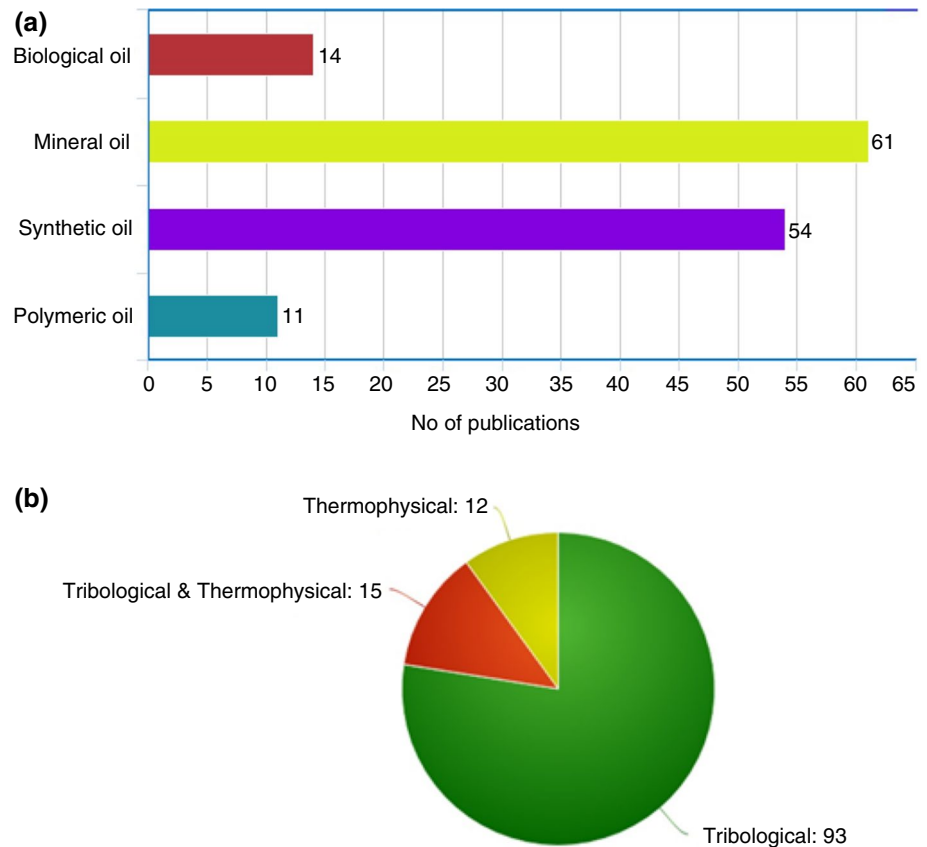
[50], carbon-coated copper [26] and (5) rare earth nanoparticles; boron nitrite [30, 51], MoS<sub>2</sub> [52–55], CeF<sub>3</sub> [56], CeO<sub>2</sub> [57], mixed rare earth naphthenate [58], Y<sub>2</sub>O<sub>3</sub> [59], TiF<sub>3</sub> [60], and CaCO<sub>3</sub> [61]. The research on nanolubricants is gaining momentum in recent years as nanolubricants provide benefits such as friction reduction, fuel economy, energy savings, and reduction in harmful emissions. By reducing the usage of high energy devices, energy can be saved which is the essential task of the society [3, 62].

The mixture of nanoparticles and any liquid (water, glycols, etc.) is called as nanofluid. The nanofluids are used in various applications, such as automobile car radiator, machining process, nuclear reactor, refrigeration and air conditioning, heat exchangers, heat pipes/pumps, heavy oil recovery, electronic cooling systems, solar collector, heating building, drug delivery systems, and pollution reduction [63–67]. Particularly, the mixture of the lubricating oil with single or composite nanoparticles is termed as nanolubricant. The various base oils used by researchers for the preparation of nanolubricants are depicted in Fig. 2a. It is clearly understood that many researchers have used mineral oil and commercial engine oil as their base lubricants compared to biological and polymeric oils. Most of the nanolubricants research studies focus on the improvement of tribological characteristics while only a few number of studies on the

enhancement of its thermo-physical properties (Fig. 2b). Also, the tribological and thermo-physical properties study of the same nanolubricant is limited. For an overall performance enhancement, a nanolubricant is required to have good tribological and thermo-physical properties, because the friction and the resulting heat have to be reduced for the improved life of the parts being lubricated. The information provided in Fig. 2 is based on the key word search nanolubricants in Science Direct data base over the period from 2016 to 2019. In the present review article, both tribological and thermo-physical properties of mono- and hybrid nanolubricants like friction, wear, thermal conductivity, kinematic viscosity, flash point, and pour point and their dependence on size, shape, nature of nanoparticle, nanoparticle concentration, and working temperature have been analyzed in detail. Challenges faced regarding the tribological properties of nanolubricants have been discussed with the help of variety of experimental research articles.

The purpose of this review article is to deliver a holistic knowledge to the readers on the thermo-physical and tribological properties of nanolubricants. Also, this review article includes the study of nanolubricants based on new nanomaterials like fly ash, halloysite clay, diesel soot, cellulose nanocrystals, etc. The detailed analysis of nanolubricant

**Fig. 2** **a** Various base lubricants and **b** Property study of nanolubricants



stability and its characterization methods is reviewed in this study.

## Preparation of nanolubricants

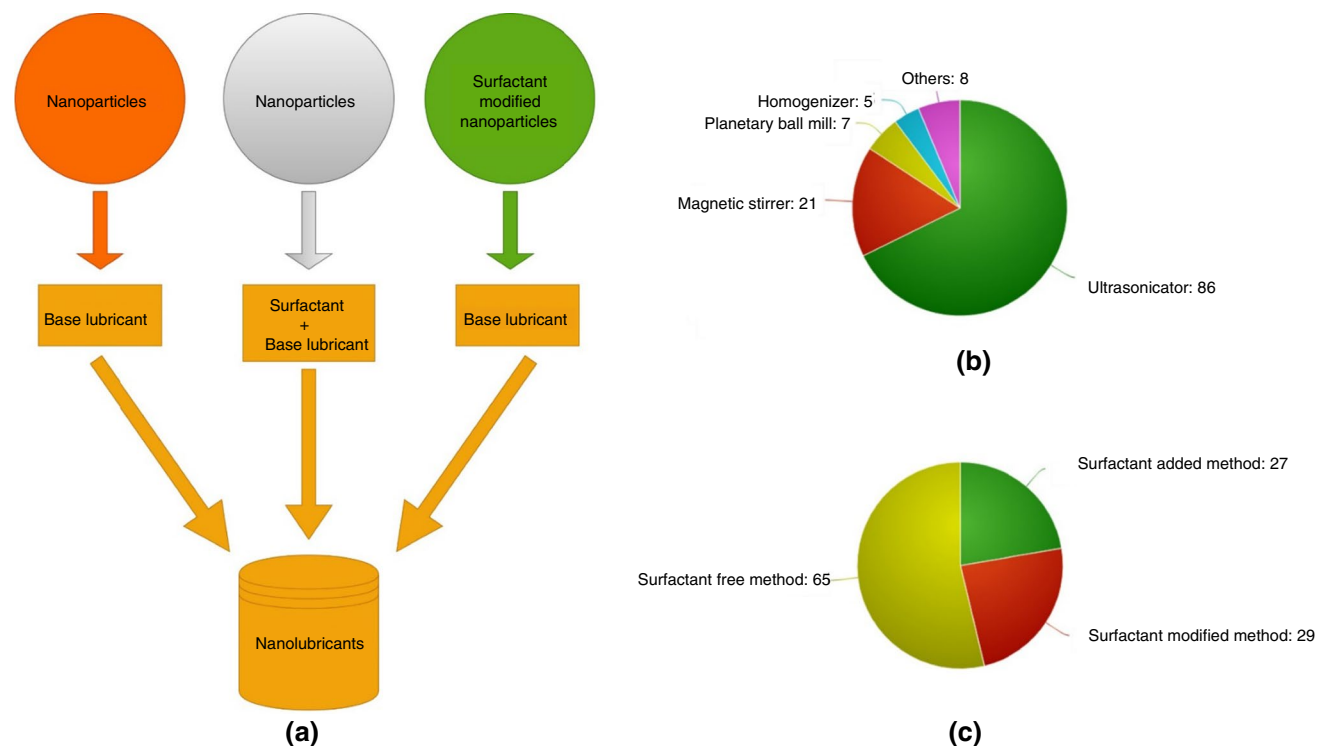
The nanolubricants are prepared in two methods, i.e., one-step method, and two-step method [68, 69]. The two-step method is the most widely used method for preparing nanolubricants. Also, two-step method is the most economical method to produce nanolubricants on a large scale. In the two-step method, synthesis of nanopowder is the first step. Chemical or physical methods produce nanopowders. Generally, available forms of nanopowders are nanoparticles, nanosheets, nanofibers, nanotubes, or other nanostructured materials [70, 71]. Following this, the nano-sized powder will be dispersed into a base lubricant, which is the second step of preparation. Figure 3b shows the data on nanolubricants preparation instruments. The nanolubricants are prepared by dispersion of nanopowder, and it is done with the help of ultrasonicator bath/probe-type [39–42, 72, 73], planetary ball milling [36, 45], mechanical stirrer [29, 49], high shear homogeneous mixer [30], stirred bead milling [32, 50], magnetic stirrer [8, 40, 51, 74], man-made agitator [75]. From Fig. 3b, it can be concluded that the most used method for preparation is ultrasonication method.

## Methods of nanolubricant preparation

Generally, three methods of compositions were used to prepare the nanolubricants [76] and statistics of previous research with respect to the three methods are depicted in Fig. 3a, c. They are,

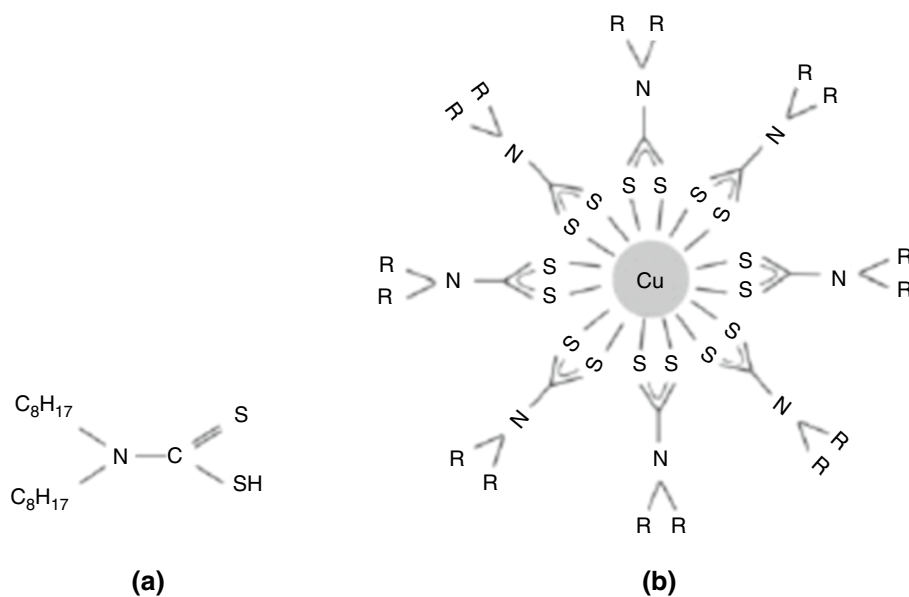
- *Surfactant free method* In this method of composition, the nanoparticles are directly mixed in base lubricants and any modified agent is not used to bind the solid (nanoparticle) surface or base lubricants.
- *Surfactant addition method* In this method of composition, surfactants are directly added in the nanoparticle and base oil mixtures.
- *Surfactant-modified method* In this method of composition, the surfactant used to modify the surface of the nanoparticles blend with base lubricants. Figure 4 shows the chemical structure of DTC8 surfactant and DTC8 surfactant-modified Cu nanoparticles).

Table 1 presents the information on different types of lubricants, preparation instruments, nanoparticle size, shape, etc.



**Fig. 3** a Corresponding design of three compositions, b corresponding instruments used on nanolubricant preparation, c corresponding statistics of three compositions on previous research)

**Fig. 4** **a** Chemical structure of DTC8. **b** DTC8-modified Cu nanoparticles [99]



## Tribological properties of nanolubricants

### Friction and wear

Many nanoparticles have been used as an additive in lubricating oil to improve its tribological properties. Appreciable number of research reports highlighted the improvement of nanolubricants tribological properties and indicated that the enhancement is influenced by various parameters such as nanomaterials, nanomaterials concentration, temperature, base oil, stability. Also, it is based on various types of mechanisms/effects (ex: sliding, rolling, bearing, tribofilm formation of nanoparticles in sliding surfaces) [76, 100]. All four type of friction reduction mechanisms were reported for all type of nanostructures. Specifically, both spherical and sheet like nanostructures undergo sliding, rolling, bearing mechanisms. The graphical diagram of friction reduction mechanisms is showed in Fig. 5.

The mechanisms/effects of nanostructures on worn surfaces are mainly characterized using SEM, TEM, EDAX, XPS, AFM, Raman spectroscopy, optical microscope, 3D-profilometer, and AFM. Particularly SEM, TEM, optical microscope, profilometer, and AFM instruments are used to know the surface morphology of the nanoparticles deposited over the sliding surfaces and wear scar diameter (WSD) of the specimen surface. At the same time, XPS, EDAX, and Raman spectrum are performed in order to examine the presence of various chemical elements, bonds, and its binding energy on the sliding surfaces.

Table 2 lists out the various instruments used for frictional worn surfaces analysis.

Further, tribological mechanisms/effects of nanostructures on worn surfaces are presented in Table 7 (refer in Appendix 1).

Different nanoparticles such as metals, metal oxides, carbon group materials, and rare earth materials exhibit various mechanisms/effects on frictional surfaces. In recent times, nanolubricants based on low cost and environmental friendly nanomaterials like cellulose nano-crystals, diesel soot, and halloysite clay nanotubes are gaining importance and the subject of research by several researchers. So, one of the objectives of this review study is to motivate and give hope to develop new low cost and environmental friendly nanomaterial-based nanolubricants by the future researchers.

Table 8 (refer in Appendix 2) enlists variety of instruments used in the study of tribological properties of nanolubricants. The instruments used are pin-on-disk, four ball tribo testers, HFRR, etc. The pin-on-disk and four ball tribometer are the mainly used tribological analyzing instruments. The pin-on-disk tribological tester finds the COF and the wear of the nanolubricants.

The four ball tribo tester is used for semi-solid lubricants like grease measures the extreme pressure in addition to friction coefficient and wear. The arrangement of pin-on-disk instrument is shown in Fig. 6.

Zhang et al. [4] investigated the friction study of Ag–MoS<sub>2</sub> hybrid nanolubricant in three lubricant regimes namely, hydrodynamic, mixed, and boundary regime (Fig. 7).

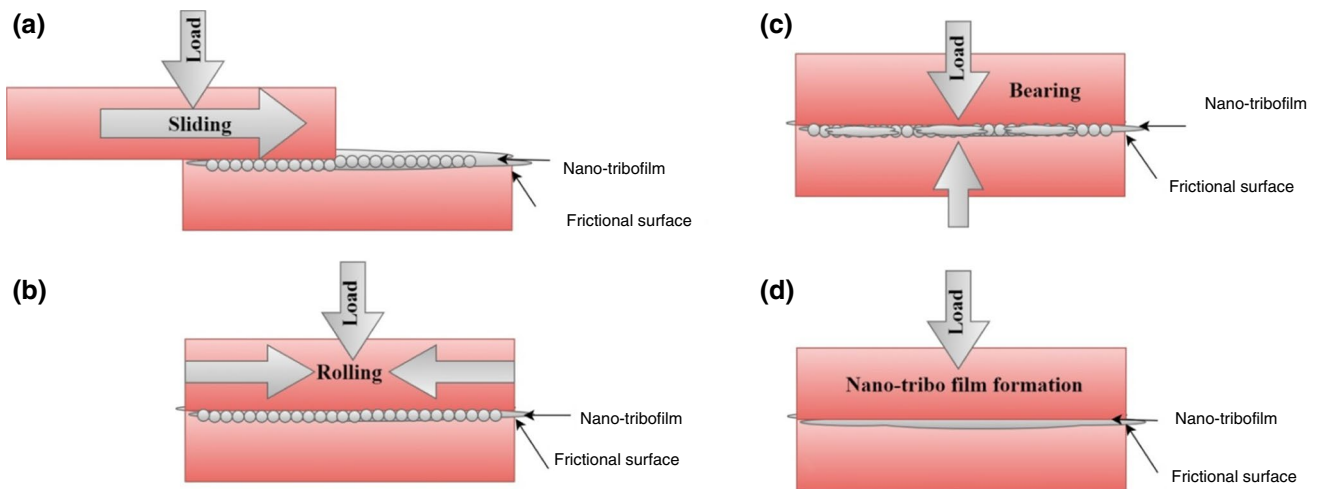
For a boundary regime, if the  $\lambda$  value is lower than 1, then it is conventionally asserted that asperity interaction becomes more severe and that the shear properties of the films on the solid surfaces, weather formed by adsorption or reaction becomes significant. If the lambda value exceeds

Table 1 Summary of various parameters on nanolubricant preparation

Nano-particle	Base lubricants	Surfactant used	Size	Structure	Concentration	Time	Instrument used	Study	References
CaCO <sub>3</sub>	50SN oil	SDS	15 nm	Spherical	0.2 to 1 mass%	–	–	Tribology	[61]
CuO	SAE20W50	–	–	–	0.1, 0.2 and 0.5 mass%	–	Planetary Ball mill and Ultrasonic bath/probe	Thermal	[77]
TiO <sub>2</sub>	SAE 10W-40, Ethylene glycol and Paraffin oil	–	59 to 220 nm	Spherical	–	10 h	Man-made agitator	Tribology	[75]
Nickel	PAO6	–	20 nm	Nearly spherical	0.5, 1 and 2 mass%	30 min	Ultrasonicator probe	Tribology	[78]
CuO	Mineral oil	–	30 to 40 nm	Nearly spherical	0.5 to 1.5 mass%	30 min and 3 h	Ultrasonicator and Planetary ball mill	Kinematic viscosity & Tribology	[79]
MoS <sub>2</sub> and SiO <sub>2</sub>	Lubricant oil	–	90 nm, 30 nm	Nano-sheet and spherical	0.2, 0.5, 0.7 and 1.0 mass%	2 h	Ultrasonic shaker	Tribology	[80]
Cu	Mineral oil and synthetic ester oil	–	10 to 30 nm	Oblong	0.3 & 3 mass%	20 min	Stirrer	Tribology	[81]
Nickel	PAO6	OA	28.5 nm	Sphere	0.025 to 0.40 mass%	–	Stirring	Tribology	[82]
SiO <sub>2</sub>	Liquid paraffin	OA	684, 420, 362, 281, 215, 140, and 58 nm	Spherical	0.05 to 0.5 mass%	30 min	Ultrasonicator	Tribology	[83]
TiO <sub>2</sub> /SiO <sub>2</sub>	Palm TMP ester	–	50 nm	Nearly spherical	0.25, 0.50, 0.75 and 1 mass%	30 min	Ultrasonicator probe	Tribology	[84]
Diamond	Mineral oil	–	5 to 10 nm	Slices	0.00125, 0.0025, 0.005 and 0.01 mass%	1 h	Ultrasonicator probe	Tribology	[85]
MoS <sub>2</sub>	PAO	–	100 nm and 500 nm	Nanotubes	5 mass%	1 h	Ultrasonicator	Tribology	[86]
CuO	Polyol ester	–	50 nm	–	0.025, 0.05 and 0.1 mass%	1 h	Ultrasonicator	Tribology	[87]
Diesel soot(3 types)	PAO 4	Span 80	20 nm to 70 nm	Spherical and elliptical	0.05 mass%	10 min and 15 min	Magnetic stirrer and ultrasonicator	Tribology	[88]
2D-boron nitride	Olive oil and Almond oil	–	100 nm	Nano-platelet	–	4 min	Planetary centrifugal mixer	Tribology	[89]
Fly ash	PAO	OA	150 to 600 nm	–	0.2 mass%	30 min	Ultrasonicator	Tribology	[90]
rGO/GO	TMPTO or PAO40	–	630 nm/60 nm	Nanosheets	0.05, 0.1, 0.25 and 0.5 mass%	4 h	Ultrasonicator bath	Tribology	[91]

Table 1 (continued)

Nano-particle	Base lubricants	Surfactant used	Size	Structure	Concentration	Time	Instrument used	Study	References
$\text{Al}_2\text{Si}_2\text{O}_5(\text{OH})_4 \cdot 2\text{H}_2\text{O}$ (halloysite clay)	Polymeric lubricant	–	30 to 70 nm/1 to 3 mm	Tubular	0.01, 0.05 and 0.10 mass%	5 min	High speed homogenizer and ultrasonicator	Tribology	[92]
Tiny CuO	PAO	–	5 nm	Spherical	0.1, 0.25 and 0.5 mass%	6 h	Magnetic stirrer	Tribology	[93]
CNC	SAE40	–	75 nm	Spherical	0.1, 0.3, 0.5, 0.7 and 0.9 mass%	2 h	Ultrasonicator	Tribology	[94]
DAG	Commercial engine oil	dodecyl amine	–	Nanosheets	0.02, 0.04, 0.06, 0.08 and 0.10 mass%	6 h	Ultrasonicator bath	Tribology	[95]
$\text{Al}_2\text{O}_3$ and $\text{SiO}_2$	Commercial gear oil	–	40 nm and 46 nm	Spherical	0.3, 0.6 and 0.9 mass%	2 h	Magnetic stirrer and ultrasonicator	Tribology, Rheology	[96]
Activated carbon (milled)	Solar glycol	Gum Arabic	–	Nano-sheet	0.2, 0.4 and 0.6 mass%	15 min and 60–90 min	Magnetic stirrer and ultrasonicator	Thermo-physical	[97]
Graphite oxide	15W-40	–	–	Nano-sheet	0.00, 0.05, 0.10, 0.15, and 0.20 mg mL <sup>-1</sup>	–	Ultrasonicator probe	Tribological	[98]



**Fig. 5** Friction reduction mechanisms; **a** Sliding, **b** rolling, **c** bearing, **d** nano-tribofilm formation

**Table 2** Frictional worn surface analyzing instruments

Instruments used	References
SEM with EDAX	[7, 10–13, 15, 24, 27, 28, 31, 33, 39, 40, 48, 49, 52, 53, 73, 78, 79, 81, 83, 86, 88, 90, 92–94, 101–112]
SEM with EDAX mapping	[113, 114]
FE-SEM with EDAX	[6, 7, 51, 82, 83]
TEM with EDAX	[4]
HR-TEM	[115]
AFM	[18, 32, 54, 57, 83, 109, 116]
SEM only	[19, 20, 29, 32, 41, 47, 51, 57, 59, 82, 84, 88, 98, 117–121]
FE-SEM only	[80]
Raman spectroscopy	[51, 88, 90, 93, 112]
XPS	[20, 22, 32, 58, 80, 82, 84, 95, 103, 111, 112, 117, 118, 122–124]
XRD	[49, 119]
3D- Profilometer	[53, 89, 91, 92, 95, 98, 105, 111, 119, 122]
Optical microscope	[93, 95, 101, 105, 125]
AES	[58]
EELS	[115]
Speckle interferometer	[126]
Not reported	[17, 21, 25, 37, 38, 43, 127]

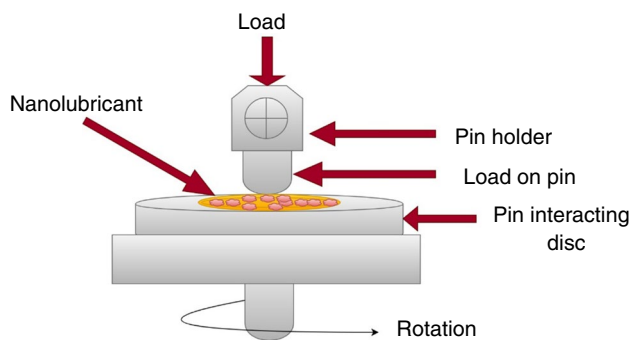


**Fig. 6** Pin-on-disk friction and wear testing machine

much higher than unity, then the film becomes thick, then the traction or friction force will be the function of bulk rheological properties of the nanolubricant under required operating conditions of load, temperature, shear rate, etc. It was found that the influence of surface roughness was negligible. This regime is said to be hydrodynamic lubrication regime. When the thickness of the film and the surface roughness are in compatible dimensions ( $1 < \lambda < 5$ ), then the friction force will still be dependent on the lubricant bulk properties, but the local contact conditions of asperity interaction are to be still taken into consideration. As the lubrication is a mixture of full film lubrication and some asperity



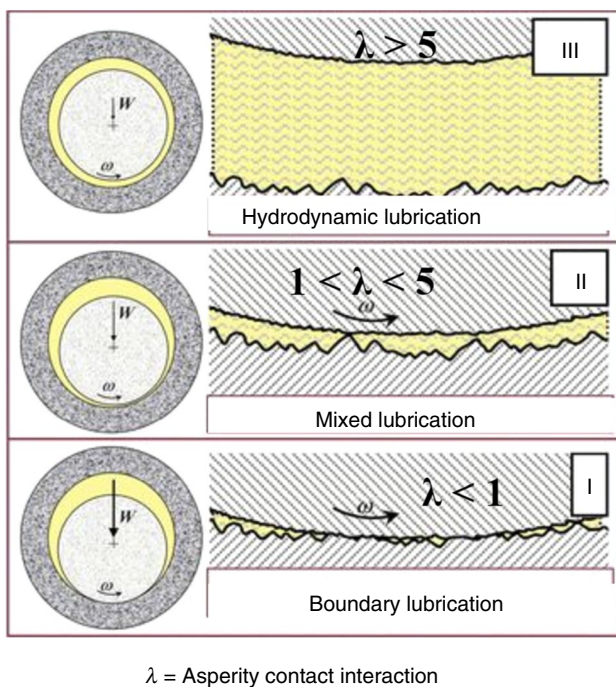


Fig. 7 Three lubrication regimes [133]

contact, the regime is called as mixed lubrication [134]. The frictional behavior of various Ag–MoS<sub>2</sub> multi-component system over a range of speeds was studied. It is clear that 2% Ag–MoS<sub>2</sub> hybrid nanolubricant sample shows significant reduction in friction during sliding at high speed hydrodynamic and mixed regimes and at very low speed boundary conditions when compared with cases of formulated oil and MoS<sub>2</sub> (molybdenum disulfide) nanoparticles. Particularly, molybdenum disulfide nanoparticles do not show frictional improvement in both hydrodynamic and mixed conditions, but when it boundary conditions are counted, MoS<sub>2</sub> molybdenum disulfide nanoparticles show considerable friction reduction (18% comparing with base oil) due to formation of a low friction tribofilm on shearing of the nanoparticles. From comparison of different concentration of Ag nanoparticles in Ag–MoS<sub>2</sub> system, it can be inferred that tribological performance is negatively influenced by increasing concentration of Ag nanoparticles which can be observed from 2%, 5% to 10% Ag samples. Although 2% Ag sample does not influence friction in hydrodynamic and mixed conditions when compared with the other Ag samples, there is a significant reduction in friction in boundary conditions. The reason for better tribological performance obtained by low Ag concentration is due to the better dispersion of silver nanoparticles in MoS<sub>2</sub> matrix, which could improve the strength of tribofilm. In addition, silver nanoparticles could be coated over by molybdenum disulfide nanoparticles because of its higher embedability. But, while high concentration Ag was tested for tribological property, higher

number of non-agglomerated silver nanoparticles were found to be dispersed outside the MoS<sub>2</sub> matrix. These free Ag nanoparticles tend to form larger agglomerated particles of silver which generally do not contribute in reduction in friction. The friction coefficient of silver is considerably higher when it exists as a thin layer of coating even though it is generally low-shear metal.

Chang et al. [7] investigated the friction and wear properties after incorporating Bi (Bismuth) and Bi/Cu hybrid nanolubricants. The concentration of Bi-based nano-oil samples are 0.05 mass%, 0.1 mass%, 0.15 mass%, 0.2 mass%, 0.5 mass%, and 1.0 mass%, and the Bi/Cu hybrid nano-oil samples are 0.02 mass% Bi + 0.08 mass% Cu, 0.05 mass% Bi + 0.05 mass% Cu and 0.08 mass% Bi + 0.02 mass% Cu. They observed 0.1 mass% of Bi nanolubricant sample reduced the friction and wear by 68.9% and 38.6%, respectively. On the other hand, 0.02 mass% Bi + 0.08 mass% Cu composite-based nanolubricants minimized the friction about 71% and 50.95% of wear compared to base oil. The highest reduction percentage in friction and wear scar diameter of bismuth nanolubricant was about 37.1% and 22.29%, respectively, for a load of 20 kgf. This reduction was accounted by rolling/sliding mechanism between the surfaces, where bismuth nanoparticles resemble as a ball or sphere. [No reports for maximum results of bi/cu hybrid].

Ali et al. [8] reported the frictional behavior of Al<sub>2</sub>O<sub>3</sub>, TiO<sub>2</sub>, and Al<sub>2</sub>O<sub>3</sub>/TiO<sub>2</sub> hybrid nanolubricant blended with oleic acid surfactant where the hybrid nanolubricant is a mixture of two distinct or coated (doped) nanoparticles mixed in base lubricants. The results showed that 0.25 mass% was the best suitable sample for the given parameters such as average sliding velocity of 0.7 m s<sup>-1</sup> and load of 160 N for 25 min. This is due to thermal conductivity improvement of all the nanolubricants (Al<sub>2</sub>O<sub>3</sub>, TiO<sub>2</sub>, and Al<sub>2</sub>O<sub>3</sub>/TiO<sub>2</sub>) from 12 to 16%. Again, a decrement in the friction coefficient of about 40–50% and about 20–30% for wear of the piston ring was observed compared to the base oil. They also explained that the nanoparticles changed the sliding friction into rolling friction, due to reduced interfacial interaction between the frictional surfaces. A tribofilm was created on rubbing surfaces. It was observed that the oleic acid alone contributed to friction reduction due to chemical reaction on worn surfaces. The average friction value was increased as the sliding velocity increased. It was observed that there was no more oxide layer formation in frictional surface, so the value of friction reduction lowered. The average wear rate value was decreased and was lower than the base lubricating oil. However, the TiO<sub>2</sub> nanolubricants showed less anti-wear/anti-friction; thus, it is evident that the wear rate minimizes on the ring with TiO<sub>2</sub> nanoparticle deposit compared to that of Al<sub>2</sub>O<sub>3</sub> nanoparticles.

Ali et al. [9] reported the anti-frictional effect of TiO<sub>2</sub> and Al<sub>2</sub>O<sub>3</sub>-based nanolubricants for an average sliding speed and

a load of  $0.5 \text{ ms}^{-1}$  and 120 N, respectively. The oleic acid (1.95 mass%) mixed engine oil sample reduced the friction of about 11%, but the overall friction reduction value using  $\text{Al}_2\text{O}_3$  and  $\text{TiO}_2$ -based nanolubricant was 45% and 50%. This reduction was observed since the  $\text{Al}_2\text{O}_3$  and  $\text{TiO}_2$  nanoparticles stucked on the specimen surface which was identified with the help of EDS. Researchers claimed that this sticking effect reduced the friction on worn surfaces. To be more specific, maximum  $\text{TiO}_2$  nanoparticles were deposited on the surface of the specimen.

Luo et al. [11] investigated the friction/wear study of KOH-560-modified  $\text{Al}_2\text{O}_3$  nanoparticles in lubricating oil. The friction reduction was about 17.61% and wear about 23.92%. A decrease by 41.75% (348.09  $\mu\text{m}$ ) was observed in the wear scar diameter compared to base lubricant (597.58  $\mu\text{m}$ ). This reduction was mainly due to the conversion of sliding to rolling mechanism in nanoparticles on frictional surfaces.

Jiao et al. [12] studied the tribological effect of  $\text{Al}_2\text{O}_3/\text{SiO}_2$  hybrid nanoparticle-blended lubricating oil at four different concentrations (0.05, 0.1, 0.5, 1 mass%), and they were named as follows; the base lubricant sample was denoted as 'A.' The  $\text{Al}_2\text{O}_3/\text{SiO}_2$  composite nanolubricants samples were named as B, C, D, and E. The results after friction test was studied were found that the sample 'A' had higher friction coefficient compared to all other samples (B, C, D, and E). Moreover, the 0.5 mass% of  $\text{Al}_2\text{O}_3/\text{SiO}_2$  hybrid nanolubricants sample showed better anti-friction effect compared to 0.5 mass% of distinct  $\text{Al}_2\text{O}_3$  and  $\text{SiO}_2$  samples. Also, they reported that the 0.5 mass% of  $\text{Al}_2\text{O}_3/\text{SiO}_2$  hybrid nanolubricants sample had better wear resistance.

Kaviyarasu and Vasanthan [43] investigated the tribological study of Cu and CuO nanoparticle-blended SAE20W40 engine oil at 0.1 and 0.05 mass% concentrations. The study revealed that the copper nanolubricants showed better performance than copper oxide nanolubricants, for example: 0.1 mass% of copper and copper oxide nanolubricants reduced COF by 58% and 27%, respectively.

Zin et al. [39] examined the tribological properties of carbon nano-horns (0.04%, 0.1%, 0.2%, 0.5%, and 1 mass%) blended PAG. The 0.1 mass% nanolubricant sample had superior performance with minimum co-efficient of friction ( $\mu$ ) only about 0.134 at room temperature (25 °C). Basically, the carbon nanostructures are best friction reducer under room temperature condition where the friction rate reduced up to 7% at 70 °C. While the 0.1 mass% concentration nanolubricant sample showed excellent friction resistance than base oil. The overall friction reduction rate was decreased by 18%. It was claimed that the carbon nano-horns are peculiar structures and it converts the sliding to rolling mechanism on frictional surface which minimizes the friction.

Zhang et al. [47] determined the tribological effects of diesel soot and graphite nanoparticle-added PAO4 oil/span

80 composition. The friction and wear study results showed that the 0.01 mass% diesel soot/PAO4 oil-based sample was better than 0.01 mass% nano-graphite/PAO4 oil. A decrease in wear rate up to 90% at 175 °C was observed for diesel soot nanolubricants. Finally, they concluded that diesel soot exhibited better wear reduction compared to graphite sample over 60 °C.

Tang et al. [48] investigated the friction and wear study of RGO-Cu nanolubricants. The test samples such as pure paraffin oil ( $S_1$ ), 1.5 mass% of copper nanoparticles ( $S_2$ ), 1.5 mass% mixture of copper nanoparticles and RGO ( $S_3$ ), and 1.5 mass% of RGO-copper nano-composite ( $S_4$ ). The working specifications of the test sample were sliding speed;  $0.025 \text{ ms}^{-1}$  and Load; 19.6–98 N. The result showed that the friction/wear reduction rate of RGO-Copper nanolubricants ( $S_4$ ) was increased with increased sliding speed and load.

Charoo and Wani [51] investigated the tribological study of h-BN/SAE20W50 nanolubricants. The results revealed that the h-BN nanolubricant exhibited excellent friction and wear reduction. The least COF value observed was 0.0401 at 3 mass% with standard load of 100 N and sliding velocity of  $0.03 \text{ m s}^{-1}$ . Further, the average reduction in wear loss was about 30–70% after adding the h-BN nanosheets to the base lubricant.

Srinivas et al. [52] reported the frictional effect of  $\text{MoS}_2/\text{SAE20W40}$  nanolubricant. The lower concentration of blended oil sample showed effective improvement than other concentrations. Even an increase in the mass fraction of 0.5 mass% resulted in no more improvement in anti-wear study. It was even observed that the enhancement of wear resistance was in between the range of 0.25–0.5 mass% at 60 kgf load.

Sunqing et al. [56] studied the tribological effect of nano- $\text{CeF}_3$ -based nanolubricants. The 0.5 mass% nanolubricants sample decreased the friction up to 26.5%. These nanoparticles form a safety tribofilm on the rough specimen surfaces. Further, the effect of friction was found to be increased as the concentration of nanomaterials increased. The study stated that the friction will be reduced only up to a certain point and then started to increase.

Thottackkad et al. [57] examined the friction and wear properties of  $\text{CeO}_2$  nanoparticles added in various type of lubricant oil such as coconut oil (0.51 mass%), paraffin oil (0.46 mass%), and engine oil (0.63 mass%). The  $\text{CeO}_2$  nanoparticles were used to modify the surfactant dodecyl succinic anhydride and tween 20. The friction/wear analysis was performed only in boundary regime. The result showed that the modified  $\text{CeO}_2/\text{coconut}$  oil samples had better friction and wear reduction in nearly 22% and 17%, respectively.

Chou et al. [78] examined the friction study of PAO6/nickel nanoparticle-based nanolubricants at three concentrations (0.5, 1 and 2 mass%). The 0.5 mass% nickel nanoparticles/oil sample showed the maximum friction reduction

up to 30%. Whereas the reduction in friction using 1 and 2 mass% of blended nanolubricant sample showed only about 7%. This reduction insisted the presence of nanoparticles being deposited on the worn surface of the specimen which was assured by SEM-EDAX.

Zhen-bing Cai et al. [88] found the friction and wear properties of different heavy vehicle diesel soot (A, B, and C) blended with Poly-Alpha-Olefin 4 oil/span 80 surfactant. The results of 1 mass% (Span 80)/soot 'A' blended nanolubricant showed significant friction reduction than base oil. The value of coefficient of friction 0.01 mass% of soot 'A' sample decreased (0.12) when compared to that of the base oil COF (0.57). However, the COF was increased between the concentrations of 0–0.001 mass%, and subsequently decreased in the range of 0.001–0.01 mass% and then remained virtually constant between 0.01 and 5 mass% concentration. The wear rate of 0.01 mass% of diesel soot/PAO4 sample observed a decrease up to 75.2%. The results suggested that the size, dispersion stability, electrochemical action, surface charge, and concentrations of diesel soot are the contributing factors for reducing the tribological properties.

Laura Reyes [89] performed an analysis on the friction of 2D boron nitride nano-plate mixed with different oils (olive oil, motor oil, and almond oil) at loads (standard for all test) of 10 and 20 N. The  $\mu$  value of pure olive oil was 0.087 and 0.176; almond oil was 0.168, and 0.187; and motor oil was 0.210 and 0.189, respectively, at the mentioned loads. The study stated that both natural oils showed prominent lubrication effects compared to synthetic motor oil, and its COF ( $\mu$ ) decreased up to 59%. The  $\mu$  value increased from 0.032 to 0.083 for the load of 10 N, and from 0.028 to 0.115 for 20 N for BNNP/olive oil. In case of  $\mu$  of BNNP/almond oil, it increased from 0.068 to 0.142 for 10 N and from 0.10 to 0.160 for 20 N. Thus, the BNNP-added olive and almond oil showed a decrease in COF up to 84%. The conventional lubricant showed higher COF (0.189) compared to almond oil with BNNP (COF=0.100) and olive oil with BNNP (COF=0.028) at 20 N load. It was mentioned that COF drastically decreases with increase in the addition of BNNP. The olive oil exhibited lower COF than almond oil due to lower oxidation rate. Further, on agglomeration of BNNP with higher COF, the almond oil tends to polymerize.

Xia et al. [90] investigated friction study of four types of fly ash-based nanolubricants. The study found that the OA modified fly ash enhanced the lubricant performance with excellent stability and tribological effect. The synergy effect of fly ash/oleic acid could act as a spacer and enhance bearing effect, so it was deposited on the worn surfaces to significantly improve the friction/wear reduction abilities. The COF and wear scar width study of MH-fly ash (modified treated) and M-fly ash (oleic acid modified) were lower than those of H-fly ash (heat treated at 500 °C) and natural fly ash (un-treated) at different load conditions. A significant

improvement of lubricant property was obtained by M-fly ash/PAO oil as it reduced the COF and wear width by 14% and 37%, respectively. This study demonstrated the M-fly ash mixed PAO oil had excellent friction/wear reduction compared to other PAO/fly ash samples.

Guzman et al. [130] reported the friction and wear properties of Cu nanoparticles mixed with two oils namely mineral oil and synthetic ester oil at concentrations of 0.3 and 3 mass%. The study was performed for various contact load, sliding speed, and heat. Both the concentrations were not considerably effective in case of synthetic oil. But, at the same time, the mineral oil blended with Cu nanoparticle-based nanolubricant had an appreciable effect on friction and wear reduction.

Pena-paras et al. [92] performed the friction and wear studies of HNTs nanoparticles dispersed in polymeric lubricant at 0.01, 0.05, and 0.10 mass%. Better tribological results were obtained for 0.05 mass% concentration and little improvements at higher concentration (0.10 mass%). The wear volume loss was decreased by 41%, 70%, and 20% and, COF was reduced by 51%, 71%, and 49% at 0.01, 0.05, and 0.10 mass%, respectively. However, they reported that there was an increase in wear scar diameter for 0.10 mass%, it was likely due to nanoparticle agglomeration. These agglomerates may form new asperities, so it causes higher friction and wear.

Alves et al. [93] performed friction and wear studies of smaller CuO nanoparticles mixed lubricants at 0.1, 0.25, and 0.5 mass% concentrations. All concentrations exhibited friction and wear reduction. The better results were obtained for 0.1 mass% concentration. But, the 0.25 and 0.5 mass% concentration showed similar friction reduction behavior. However, the tiny CuO nanoparticles offered more wear reduction compared to friction reduction. Further, the 0.1 mass% CuO nanolubricant exhibited better anti-wear property compared to all other concentrations considered.

Awang et al. [94] studied the friction and wear properties of CNC-based lubricant prepared at 0.1, 0.3, 0.5, 0.7, 0.9 mass% concentration. An excellent friction/wear reduction was achieved due to the deposition and tribo-chemical reaction of CNC nanoparticles. The 0.1 mass% concentration results showed better reduction in COF compared to other concentration of CNC nanolubricant, as well as, 0.1 mass% performed better in both conditions (500 rpm—39.24 N and 200 rpm—98.1 N). Further, the 0.5 mass% nanolubricant exhibited minimum friction reduction compared to all other concentrations considered. Interestingly, 0.1 mass% observed maximum wear reduction up to 69% for 200 rpm—98.1 N test condition.

Kotia et al. [96] studied the friction/wear properties of  $\text{Al}_2\text{O}_3$ - $\text{SiO}_2$ /gear oil-based nanolubricants at three various concentrations (0.3, 0.6, 0.9 mass%). The results showed 25% and 22% of friction reduction and an improvement of 127% and 88% in the anti-wear performance for 0.3 mass%

$\text{Al}_2\text{O}_3$ /gear oil and 0.3 mass%  $\text{SiO}_2$ /gear oil nanolubricant, respectively. The results indicated that 0.3% volume fraction is a limiting particle concentration, and also ball-bearing effect was the controlling mechanism for the sliding surface. However, the EDS result suggested that silica nanoparticles were contributing to effect of surface polishing, in addition to the ball-bearing effect. They claimed that the dispersion of  $\text{Al}_2\text{O}_3$  nanoparticles in gear oil produces more beneficial results as compared to  $\text{SiO}_2$  nanoparticles.

Naveen Kumar et al. [111] investigated the friction and wear study of prepared lubricants like LUB-1 (0.5 mass% micro- $\text{MoS}_2$ ), LUB-2 (0.5 mass% nano- $\text{MoS}_2$ ), and LUB-3 (0.5 mass% Ni promoted  $\text{MoS}_2$  nanosheets) against the base gear oil (SAE75W). The friction coefficient of LUB-3 was better than the other two lubricants (LUB-2 and LUB-1). The LUB-1 showed lower friction compared to gear oil. Similarly, LUB-1 friction reduction was higher compared to that of LUB-2 and LUB-3 due to its flake-like structure and agglomerated size leading to sticking wear. These results indicated that the lubricant film thickness between the asperities decreased with an increase in the load, size, and shape of the  $\text{MoS}_2$  particles. On the other hand,  $\text{MoS}_2$  nanosheet-based gear oil was easily mending and gives plastic deformation due to the impact of contact pressure. However, LUB-2 possessed better effects of anti-wear compared to LUB-1 and gear oil, but not better than LUB-3. The results assured that the LUB-1 was not exhibiting any continuous film formation. So, large amount of micro-crack and metal burrs were observed over the sliding surfaces. Whereas, the LUB-2 was patch up and filled the cracks and burrs over the frictional surfaces. However, the LUB-3 completely eliminates metal burrs and grooves and exhibited the linear boundary effect compared to other lubricants. Moreover, they mentioned that the increase in number of Mo and S elements deposited over the worn surfaces enhances the reduction in friction and wear with LUB-3 combination which was higher than LUB-2 and LUB-1 combinations.

Overall, nature of bonding energy determines the performance of nanolubricants. The non-polar characteristics contained nanostructures exhibited higher bonding energy. Nano-polar contained nanostructure-based nanolubricant showed excellent friction/wear reduction rate than polar nanostructures such as carbon nanostructure since it mostly contains non-polar functional group [135, 136]. Because, nanoparticles with higher bonding energy provide better load-bearing effect between the two surfaces [72].

The functional group and binding energy analysis (FTIR, XPS) of the nanostructures are most important in tribological and thermo-physical (kinematic viscosity, flash point and pour point) study of nanolubricants. Because, functional groups are most crucial role of nanolubricant study. But still less numbers of nanoparticles functional group analysis study were investigated and reported. The number

of nanolubricant study without and with FTIR and XPS analysis over a period from 2009 to 2020 is shown in Fig. 8.

## Thermo-physical properties of nanolubricants

Thermo-physical properties play an important role in lubrication process. Increase in lubricant temperature affects the thermo-physical properties. Researchers reported that the nanolubricants generally offer higher thermal conductivity and viscosity compared to conventional lubricants which could help resolve the heat transfer problems on inner part of the systems. Instruments used to measure thermo-physical properties of nanolubricants are presented in Table 3.

### Thermal conductivity

In a complex system, such as a nanofluid, it is possible that a combination of mechanisms may be responsible for the enhancement in thermal conductivity and such combination of mechanisms may be specific to a nanoparticle–fluid system. As heat transfer in solid/liquid suspension occurs at the particle–fluid interface, an increase in the interfacial area can enhance to more efficient thermal transport properties. As the particle size decreases, the surface to volume ratio increases, which leads to large enhancement in the thermal conductivity of the fluid since heat transfer is a surface phenomenon. The presence of an interfacial layer may play a role in heat transport, but it is unlikely to be the only reason for the thermal conductivity enhancement. Nanoparticle exhibits Brownian movement when suspended in a liquid. As a result of Brownian motion, the fluid molecule in the immediate vicinity creates a locally ordered micro-convection effect around each particle within the base fluid [137, 138]. It is believed, that this ordered arrangement of molecule leads to heat transfer enhancement in the fluid. Therefore, adding nanoparticles to the fluid results in two possible effects-higher thermal conductivity enhancements

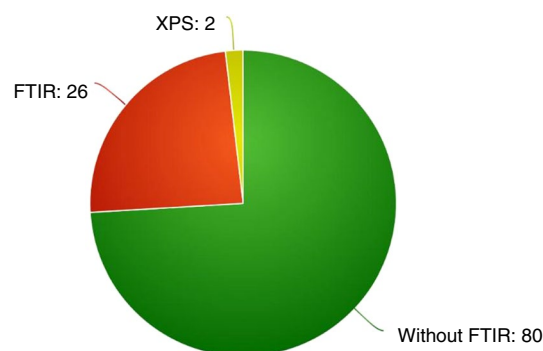
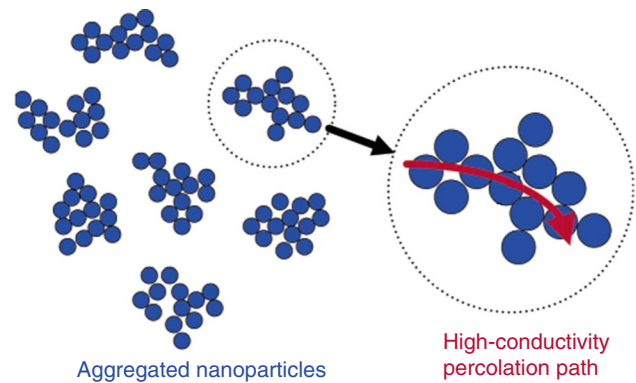


Fig. 8 Progress of FTIR and XPS analysis in nanolubricant study

**Table 3** Instrument details for measuring thermo-physical properties

Thermo-physical property	Instrument used
Thermal conductivity	KD2-Pro thermal property analyzer (Decagon Devices, USA) [5, 8, 14, 16, 36, 42, 43, 45]
Kinematic viscosity	Rheometer (Anton-Paar, Austria) [5] ASTMD-445 0.26% [36, 42, 54] LVDV-III (Low Viscosity Digital Viscometer-III) Ultra Programmable viscometer [14]
Flash point	Pensky–Martens open cup apparatus as per ASTM D6450 [5] ASTMD-92 $\pm 8$ °C [36, 42, 54, 77]
Pour point	ASTMD-97 $\pm 3$ °C [36, 42, 77]

due to formation of highly ordered arrangement of molecule around each particles and the other effect is the stirring action caused by Brownian motion of the particles. As the particles size decreases, the motion becomes larger that could contribute to larger thermal conductivity enhancement [139]. Therefore, least scale nanoparticles are better for maximum enhancement of thermal conductivity of the base fluid. Currently, it is believed that thermal conductivity enhancement in a colloidal dispersion is mainly due to micro-convection caused by the Brownian motion of the nanoparticles and aggregation of nanoparticles causing a local percolation [137]. The probability of aggregation increases with decreasing particle size, at constant volume fraction, because the average inters particle distance decreases, making the attractive Vander Waals force more important. Nanoparticles aggregation will decrease the Brownian motion due to the increase in the density of the aggregates, whereas it can increase thermal conductivity due to percolation effects in the aggregates, as highly conducting particles touch each other in the aggregate. Due to it is possible that a combination of mechanisms may be responsible for the observed enhancement and such combination of mechanisms may be specific to a nanoparticle-fluid system, one is Brownian motion is likely to be negligible as the average nanoparticle agglomerated size is large enough to effectively participate in random motion (low viscous fluids). Besides, the Brownian motion of these agglomerates is further retarded due to the inherently high viscosity of gear oil at room temperature. Nanoparticles with much higher thermal conductivity compared to base oil, the presence of nanoparticle clusters, or percolating clusters (Fig. 9) in nanolubricant create lower thermal resistance paths for efficient propagation of phonons across the oil. There is a close proximity of the nanoparticles due to the formation of percolating structures, so, heat transport due to the ballistic transport of phonons across the small gaps between particles may contribute toward substantial enhancement in thermal conductivity. Thermal conduction in nanoparticles is assumed to be ballistic (missile path) in nature, which is associated with the large phonon mean-free path in the nanoparticles. Basically, ballistic conduction of heat is much faster than thermal diffusion. The combined

**Fig. 9** Schematic diagram of well-dispersed aggregates [142]

contribution of interfacial layers, nanoparticle clusters, and the ballistic transport of phonons appears to be the possible reasons for the observed thermal conductivity enhancement in nanolubricant [140, 141].

Thermal conductivity of nanolubricants varies with temperature and is affected by opposite polarity configuration of the molecules. The thermal conductivity of most of the mineral and synthetic-based lubricants is in the range between 0.14 W/mK at 0 °C and 0.11 W/mK at 400 °C [1]. This shows that the thermal conductivity of base lubricants decreases with increase in temperature. On the other hand, thermal conductivity increases with increase in temperature of nanolubricants. In general, thermal conductivity ratio depends upon the nature of fluid viscosity.

Kumar et al. [5] investigated the thermal conductivity of Cu–Zn nanoparticle-dispersed oils (vegetable oil, paraffin oil, SAE oil) at 30 °C. The thermal conductivity was found to be increasing with increase in Cu–Zn nanoparticle concentration. In this research, the vegetable oil-based nanolubricant showed better thermal conductivity enhancement than paraffin oil and SAE oil nanolubricants.

Ali et al. [8] measured the thermal conductivity of  $\text{Al}_2\text{O}_3$ ,  $\text{TiO}_2$ , and  $\text{Al}_2\text{O}_3/\text{TiO}_2$  nanoparticle-based hybrid nanolubricants. The thermal conductivity increased with increasing temperature, due to weak cohesive forces among the oil layers at high temperature. As nanolubricant

temperature increases, the dispersion of nanoparticles was more in base oil which increased the thermal conductivity. The  $\text{Al}_2\text{O}_3$ ,  $\text{TiO}_2$ , and  $\text{Al}_2\text{O}_3/\text{TiO}_2$  nanolubricants thermal conductivity increased by 12–16%, for a temperature range between 10 and 130 °C at 0.25 mass%. The  $\text{Al}_2\text{O}_3/\text{TiO}_2$  hybrid nanolubricant showed the most significant enhancement in thermal conductivity; this enhancement is mainly due to the Brownian movement of the nanoparticles with rise in temperature and significant reduction in the thermal interface resistances between the nanoparticles, providing a rapid thermal path between nanoparticles. Generally, the  $\text{TiO}_2$  nanolubricant showed higher thermal conductivity than  $\text{Al}_2\text{O}_3$  nanolubricant, even though  $\text{TiO}_2$  nanoparticle has low thermal conductivity compared to  $\text{Al}_2\text{O}_3$  nanoparticle. The reason behind is the phenomenon of clustering of  $\text{TiO}_2$  nanoparticles in the engine oil. The  $\text{TiO}_2$  nanolubricant showed lower dispersion with time than that of  $\text{Al}_2\text{O}_3$  nanolubricants due to slight agglomeration of the  $\text{TiO}_2$  nanoparticles in the engine oil. This can easily result in the creation of channels for thermal waves and fast transport of heat resulting in an enhancement in thermal conductivity of the  $\text{TiO}_2$  nanolubricant in comparison with the  $\text{Al}_2\text{O}_3$  nanolubricant. Thus, the formation of these nanoparticle clusters tend to enhance the thermal conductivity of the nanolubricant.

Kaviyarasu and Vasanthan [43] studied the thermal conductivity of copper and copper oxide nanoparticles/SAE20W40-related nanolubricants. According to the study, 0.1 mass% and 0.05 mass% copper nanoparticle increased the oil thermal conductivity by 4.2% and 2.8%, respectively. Whereas, the copper oxide nanolubricant (0.1 mass% and 0.05 mass%) concentrations increased the oil thermal conductivity only by 2.1% and 0.7%, respectively.

Forbod et al. [16] examined the thermal conductivity of CuO nano-rhombic/nano-rod structure-based nanolubricants (0.2, 0.5, 1, 4 and 6 mass%) at the temperature of 25 °C. They said that thermal conductivity increases with increase in temperature. The maximum thermal conductivity enhancement was about 8.3% at 6 mass% CuO nano-rod structure-based nanolubricants. Finally, they reported that 4 mass% nano-rhombic structure-based lubricant had the maximum and minimum level of increase in thermal conductivity.

Ettefaghi et al. [36] analyzed the thermal conductivity of four carbon nanostructures (MWCNTs, G, CNB<sub>s</sub>, and C<sub>60</sub>)-blended SAE20W50 engine oil (Fig. 10).

The thermal conductivity of various carbon nanostructure-based nanolubricants showed significant improvement than base oil. Generally, carbon-based nanostructure materials had the highest thermal conductivity enhancement. Therefore, thermal conductivity of CNB<sub>s</sub> blended oil showed 18% increase, but C<sub>60</sub>-blended oil showed low thermal conductivity enhancement.

Ettefaghi et al. [42] conducted a study on thermal conductivity of MWCNT<sub>s</sub>-based nanolubricants. The thermal

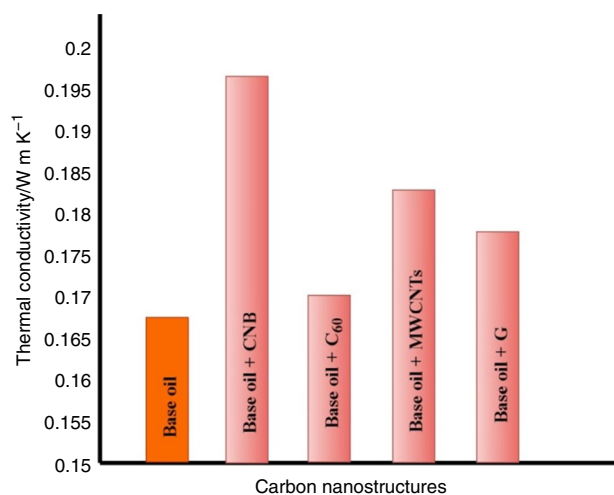


**Fig. 10** Thermal conductivity of nanolubricants for various carbon nanostructures

conductivity of prepared nanolubricants was found to be significantly improved than base oil. As the concentration increased; the thermal conductivity also increased. The thermal conductivity of MWCNTs nanolubricant at 0.1, 0.2, and 0.5 mass% increased by 13.2%, 18%, and 22.7% compared to the base oil, respectively. The 0.1 mass% nanolubricants showed excellent stability with better thermal conductivity.

Ettefaghi et al. [77] carried out the thermal conductivity study of CuO-blended nanolubricants. The thermal conductivity increased in all CuO concentration added lubricants, but the increment was only for 3%. They said that thermal conductivity enhancement was depending on change in the concentration of nanoparticles.

Naveen Kumar et al. [111] determined the thermal conductivity of Ni-MoS<sub>2</sub>-based gear oils (Oil-1, Oil-2, and Oil-3). The thermal conductivity of base gear oil (0.13 W/mK @30 °C and 0.12 W/mK @100 °C) decreased with an increase in the temperature because of large cluster chain formation with high density. Thus, higher energy exchange is necessary between the oil layers at high temperatures. On the other hand, the thermal conductivity of Oil-1 (MoS<sub>2</sub> micro-sheets/0.17 W/mK @100 °C) increased with increase in temperatures compared to base oil. Even though, Oil-1 provides high thermal conductivity compared to base oil, it is not superior in conductivity compared to Oil-2 (MoS<sub>2</sub> nanosheets) and Oil-3 (Ni-MoS<sub>2</sub> nanosheets). Since, the stability is one of the parameters for increasing the thermal conductivity. The thermal conductivity enhancement of Oil-2 and Oil-3 was 12% and 50% compared to Oil-1. They reported that the thermal conductivity enhancement in Oil-3 can be correlated with the clustering effect. However, the addition of Ni had not performed in synergy effects with MoS<sub>2</sub> nanosheets.

Thermal conductivity of nanolubricants is in direct relationship with nature of nanostructures and its concentrations. Particularly, conducting and semiconducting nanostructures increase thermal conductivity of base lubricant. It should be noted that increase in thermal conductivity was not the same as the increase in other nanolubricant properties like friction/wear, kinematic viscosity, flash point, and pour point due to the addition of nanostructures.

### Kinematic viscosity

The term viscosity is the measure of fluids' resistance to flow. Kinematic viscosity is defined as the ratio of dynamic viscosity to the fluid density [8, 9, 36, 42, 77].

$$v = \eta / \rho$$

$$v = \text{kinematic viscosity (m}^2 \text{ s}^{-1}\text{);}$$

$$\eta = \text{dynamic viscosity (Ns m}^{-2}\text{);}$$

$$\rho = \text{fluid density (kg m}^{-3}\text{)}$$

Viscosity index (VI) is an entirely empirical parameter that compares the kinematic viscosity of the lubricant of interest to the viscosities of two reference lubricant that have a considerable difference in sensitivity to temperature [2].

$$VI = (L - U) / (L - H) * 100$$

Commonly, the kinematic viscosity of the oil of the nanolubricant is measured at 40 °C and 100 °C. The value of 'U' indicates kinematic viscosity of the oil at 40 °C, and 'L' and 'H' correspond to the oils kinematic viscosity at 40 °C, having similar viscosity at 100 °C as that of the oil whose viscosity index is required. The values of *L* and *H* values are obtained from ASTM D2270. Substituting the obtained values of 'U', 'L,' and 'H' into the above equation yields the viscosity index [2].

Ali et al. [8] studied the kinematic viscosity of 0.25 mass% Al<sub>2</sub>O<sub>3</sub>, TiO<sub>2</sub>, and Al<sub>2</sub>O<sub>3</sub>/TiO<sub>2</sub> hybrid nanolubricants at the temperature of 40 °C and 100 °C. The kinematic viscosity slightly decreased than base oil. Because of this decrement, there was a relative movement of nanoparticles between the lubricant oil layers. The Al<sub>2</sub>O<sub>3</sub>, TiO<sub>2</sub>, and Al<sub>2</sub>O<sub>3</sub>/TiO<sub>2</sub> hybrid nanoparticles acted as a reducing catalyst, so the kinematic viscosity and heat transfer properties were reduced. The study stated that the increase in working temperature increased the kinematic viscosity. It may be associated with the lower forces between the oil layers. Furthermore, the 0.25 mass% oil reduced the hydrodynamic friction between the piston ring and cylinder liner. Moreover, the viscosity index increased by 2% than base lubricant. The increased viscosity index indicated a more stable kinematic viscosity with temperature change, which provided better resistance to thinning and film strength retention under conditions of

heat application. Furthermore, the addition of Al<sub>2</sub>O<sub>3</sub>, TiO<sub>2</sub>, and Al<sub>2</sub>O<sub>3</sub>/TiO<sub>2</sub> hybrid nanolubricants suppressed the rate of reduction in kinematic viscosity with an increase in temperature making the engine oil more opt for high temperature.

Ali et al. [9] examined the kinematic viscosity of oleic acid surfactant with Al<sub>2</sub>O<sub>3</sub> and TiO<sub>2</sub> nanolubricants for the temperature of 40 °C and 100 °C at 0.25 mass% nanoparticles concentration. The kinematic viscosity slightly decreased. Due to this viscosity reduction, it was easy for nanoparticles to enter between the oil layers and the TiO<sub>2</sub> and Al<sub>2</sub>O<sub>3</sub> nanoparticles acting as a catalyst. Moreover, the spherical structure of the nanoparticles played an important role in rheological behavior. At the same time, viscosity of oleic acid blended engine oil was decreased only by few percentages. The low viscosity reduction helped to reduce viscous friction. Also, the less viscosity reduction in the nanolubricants confirmed the Al<sub>2</sub>O<sub>3</sub> and TiO<sub>2</sub> nanoparticles affect alone for minimizing asperities friction, and thus reducing the frictional power losses. Moreover, the viscosity index of nanolubricants was increased by 1.84% compared to base lubricants. The increased viscosity index indicated that it provided a better resistance to thinning of the lubricant film and fuel economy for automotive engine.

Ettefaghi et al. [36] investigated the kinematic viscosity of various carbon nanostructures (CNBs, C<sub>60</sub>, MWCNTs, G) related nanolubricants with 0.1 and 0.2 mass% at the temperature of 40 °C and 100 °C (Fig. 11). They said that change in nanolubricants kinematic viscosity is based on the change in concentration of nanoparticles and temperature. The results of kinematic viscosity showed that the graphene nanosheets added oil sample had higher increment than other (CNBs, C<sub>60</sub>, MWCNTs) carbon nanolubricants.

However, the kinematic viscosity of 0.1 mass% of graphene nanolubricant exhibited very low increment compared

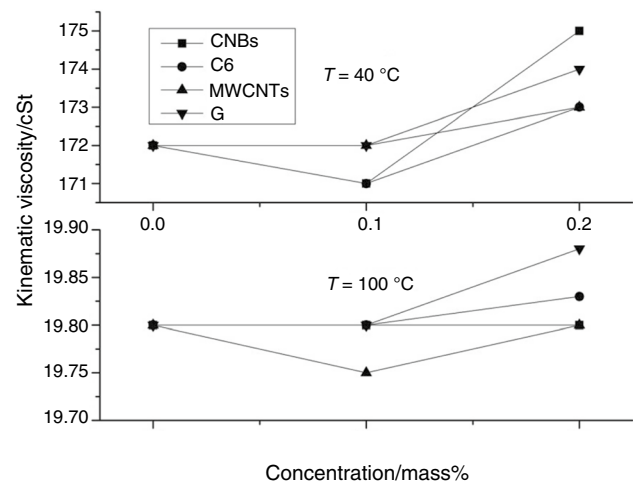


Fig. 11 Kinematic viscosity of various carbon-based nanolubricants at 40 °C and 100 °C

to base lubricant. They said that when low concentrations of spherical and tubular nanostructures are added to the oil, the nanostructures easily enter between the lubricant layers and its kinematic viscosity was slightly decreased. At the same time, the graphene (G) is a sheet-like structure, and its viscosity was not decreased. However, at increased concentration, graphene nanosheets became agglomerated and created larger uneven size of nanoparticles. So, it was interfering with the movement of oil layers and thus increased the viscosity. They concluded that the carbon nanoparticles concentration played a key role in nanolubricants viscosity.

Ettefaghi et al. [42] determined the kinematic viscosity of MWCNTs-based nanolubricants at the temperature of 40 °C and 100 °C for 0.1, 0.2 and 0.5 mass% concentrations. Basically, as the temperature increases, the viscosity of all the samples is decreased. At the same time, as the carbon nanotubes concentration was increasing, the value of viscosity was increasing. They said that kinematic viscosity of nanolubricant of 0.1 mass% had small decrement compared to base lubricant at both temperatures. Generally, when the nanotubes are added in oil, they were placed between oil layers and led to ease of movement of fluid layers between each other, and its results showed that the viscosity slightly decreased. As the mass% increased, nanotubes forms clustered and created large asymmetric particles, preventing movement of oil layers on each other; hence, viscosity was increased. Typically, the nature of the kinematic viscosity was influenced by fluid type, purity of nano-additives, concentrations, method of preparation, surfactants, etc. The kinematic viscosity was reduced by 0.25% at 100 °C for 0.1 mass%. On the other hand, the 0.5 mass% witnessed an increase by 1.7% at 40 °C.

Ettefaghi et al. [77] studied the kinematic viscosity of copper oxide nanolubricants for the concentrations of 0.1, 0.2, and 0.5 mass% at the temperatures of 40 °C and 100 °C. The kinematic viscosity of CuO nanolubricants was increased with increasing the concentration of nanoparticles at both temperatures. The 0.5 mass% CuO added nanolubricants increased the viscosity to a maximum level of 5.7% compared to the base lubricant at 40 °C. Further, 0.1 mass% copper oxide nanolubricants viscosity slightly decreased at both the temperatures of 40 °C and 100 °C. As the nanoparticle concentration was increased, the particles became agglomerated and large asymmetric particles were interfering with the oil layers' movement, so viscosity increased. Finally, they concluded that there was no appreciable change of viscosity of lubricants containing CuO nanoparticles at lower concentrations.

Naveen Kumar et al. [111] investigated the kinematic viscosity of Ni-MoS<sub>2</sub> nanosheets and MoS<sub>2</sub> micro-sheets blended with gear oil. They noted that viscosity of the lubricants mainly depended upon operating temperature as well as the size, shape, and aggregation of the particles.

Researchers reported that the kinematic viscosity of the base lubricant was lower than nanoparticle-blended gear oil, due to decrement in intermolecular forces and Newtonian behavior. In this study, the LUB-1 provides the maximum kinematic viscosity at temperature 40 °C and also found to decrease significantly at 100 °C compared to MoS<sub>2</sub> nanosheet-blended gear oils namely LUB-2 and LUB-3, and it may be due to the large size and poor suspension stability of bulk MoS<sub>2</sub>. Moreover, they said that the temperature increment of LUB-1 was indicating the failure of percolating microstructures. So, it was not stable for a long time. At the same time, LUB-2 and LUB-3 provides stable and uniform kinematic viscosity compared to LUB-1 and base oil. However, the LUB-3 attained a maximum viscosity at 100 °C compared to other lubricants. The nanoparticle concentration and temperature directly affects the viscosity of lubricants and alters the rheological behavior from Newtonian to non-Newtonian. The viscosity index of LUB-3 (Ni-MoS<sub>2</sub> nanosheets) increased nearly by 17%, which attained a maximum viscosity index compared to LUB-2 and LUB-1. They stated that Ni-MoS<sub>2</sub> nanosheets could enhance the performance of gear oil, which could lead to an improved fuel economy and provide high shearing behavior at an elevated temperature.

Technically, nanolubricant containing large C-H/alkanes molecular chain showed higher viscosity index [143]. Generally, non-polar functional group with higher surface to volume ratio contained carbon nanostructures provide extra C-H/alkanes molecular chain in base lubricant, improving the nanolubricants viscosity index. The researchers also used surfactants like oleic acid and oleylamine for forming alkanes functional group in lubricant study. The kinematic viscosity of single and hybrid nanolubricants is influenced by factors like base lubricant, nanoparticle concentration, purity of nanomaterial, nature of nanomaterial, surface area of nanoparticle, surfactants, temperature, and nanoparticle agglomeration. Moreover, shape of the nanoparticles (ex: cylindrical, rod, etc.) also influences the viscosity of nanolubricants. Nanofluids containing tube-shaped nanoparticles comparatively showed enhanced viscosity than that of spherically shaped nanoparticles [66]. The readers can find more details on the critical factors affecting the viscosity of hybrid nanofluids such as temperature, particle concentration, pH value, particle size, and morphology in Ref. [66].

## Flashpoint

The temperature at which lubricant vapor will ignite is the flash point of the lubricant. It can be measured by heating the lubricant at standard pressure to a temperature which is high enough to produce sufficient vapor to form an ignitable mixture with air [2, 5, 16, 36, 42, 77].



Kumar et al. [5] studied the flashpoint of Cu–Zn hybrid nanoparticle added to various base oils (paraffin oil, vegetable oil, and SAE 20 oil). As the concentration of hybrid nanoparticles increased, the flash point of all nanolubricants was increased. The flash point of vegetable oil-based nanolubricants had a maximum increment than other nanolubricants. They found that hybrid Cu–Zn nanoparticle was only effective on vegetable oil-based nanolubricants.

Farbod et al. [16] investigated the flash point of CuO nanostructures (nano-rhombic, nano-rod, and agglomerated nanoparticles)-based nanolubricants at 0.1 and 0.2 mass% concentration. They observed that the flash point of CuO agglomerate and nano-rhombic structure-blended lubricants was steadily increased with increasing concentrations. However, the flash point of 0.2 mass% copper oxide agglomerate and nano-rhombic structure nanolubricants increased when the temperature was 15 °C and 38 °C compared to base oil.

Ettefaghi et al. [36] investigated the flash point of various carbon nanostructures such as MWCNTs, G, CNBs, and C<sub>60</sub>/SAE 20W50 nanolubricants (Fig. 12). They found that the flash point increased for all carbon nanostructures. And it was also found that the flash point had direct relationship with the concentration of nanostructures.

On the other hand, the increase in flash point values was not linear with change in concentration. The increased flash point in nanolubricants increased the thermal resistance against ignition. Specifically, the CNB particles offered extremely high thermal resistance in engine oil. The flash point value of carbon nano-ball was higher than other samples. At the same time, flash point value of C<sub>60</sub> and MWCNT depends on the concentration of nanoparticles and MWCNT has higher flash point as compared to C<sub>60</sub> at higher concentration. The maximum increase in flash point was about 13.8% at 0.2 mass%. Thus, the carbon nano-ball particles

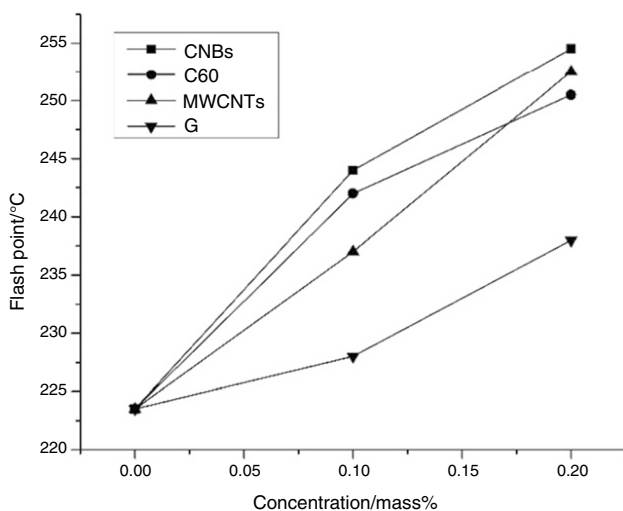


Fig. 12 Flash point of various carbon-based nanolubricants

had an effect on the flash point value of SAE 20W50 grade engine oil than other carbon nanostructures.

Ettefaghi et al. [42] determined the flash point of MWCNTs-based nanolubricants at 0.1, 0.2, and 0.5 mass% concentrations (Fig. 13).

The maximum increase in flash point was about 13% at 0.2 mass%. Moreover, 0.1 mass% and 0.5 mass% of nanolubricants had higher flash point than base oil. Finally, they claimed that 0.2 mass% of nanolubricant was better than other two concentrations of nanolubricants.

Ettefaghi et al. [77] investigated the effect of flash point of CuO nanolubricants. They observed that thermal conductivity of CuO nanolubricant was increased subsequently an increase in the value of flash point. So, it increased the anti-ignition time of nanolubricant. Furthermore, the flash point increment was directly related to the nanoparticle concentrations, although this increase was not linear. The flash point of 0.1 mass% copper oxide nanolubricants was increased by 7.5% compared to base lubricant, whereas the flash point had a maximum increase (13%) for 0.5 mass%.

Flash points are very important from a safety point of view since they constitute the only factor that defines the fire hazard of a lubricant. In general, flash point of oils increases with increase in the nanoparticles concentration. Specifically, as the required thermal energy for depletion of non-polar covalent bond is high, non-polar covalent bond (strongest bond)-containing nanostructures blended lubricant have higher flash point.

## Pour point

The lowest temperature at which the lubricant will just flow when it is cooled is the pour point of lubricant. The highest rate of wear in an engine is observed at the first moment

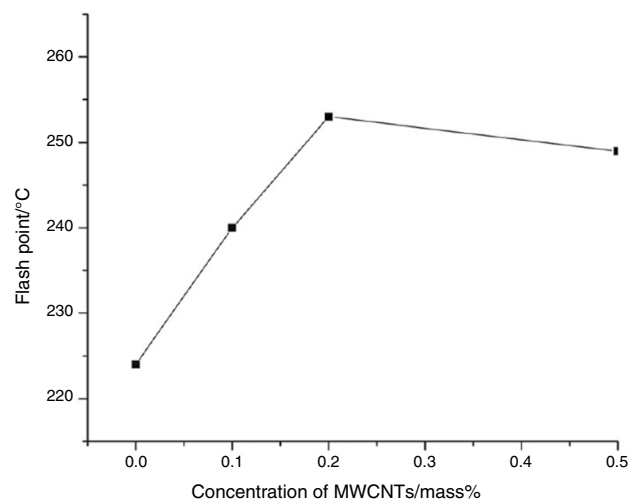


Fig. 13 Flash point of MWCNTs-based nanolubricants

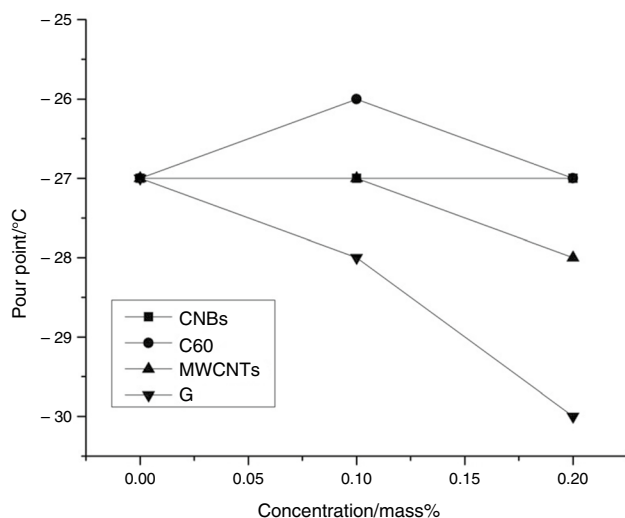


Fig. 14 Pour point of various carbon-based nanolubricants

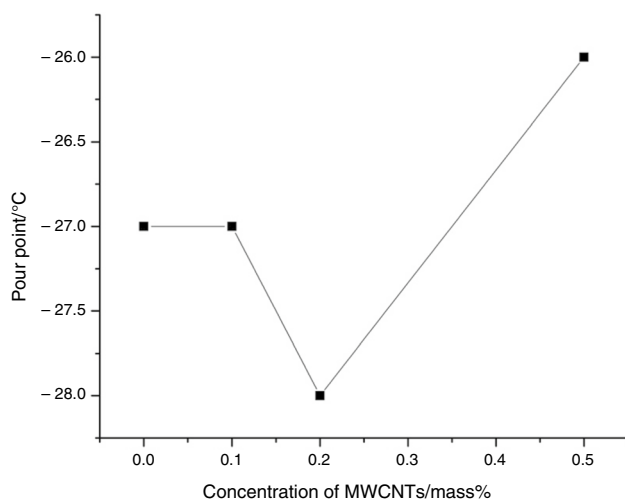


Fig. 15 Pour point of MWCNTs-based nanolubricants

when engine starts to work due to insufficiency of oil to reach all parts of the engine. To avoid this problem and to reduce its effect, it is required that the oil should be easy to pump and flow. This property of oil is evaluated with a parameter called pour point [2, 36, 42, 77].

Ettefaghi et al. [36] studied the pour point of various nanostructure-based nanolubricants (Fig. 14). The results showed that the pour point of graphene nanolubricants increased by 11% for 0.2 mass%. Generally, the carbon nanostructures have an excellent effect on lubricants. But, it was reported that there was no substantial effect in pour point study.

Ettefaghi et al. [42] investigated the pour point of MWCNT<sub>S</sub> nanolubricant at three concentrations (Fig. 15).

The 0.1 mass% MWCNTs nanolubricants showed no change in pour point. However, for 0.2 mass% MWCNT<sub>S</sub> nanolubricant, it increased by 7.4%. But, for 0.5 mass% MWCNTs nanolubricant, it was found to be decreased.

Ettefeghi et al. [77] carried out the pour point study of CuO-based nanolubricants (0.1, 0.2, 0.5 mass% concentrations). The pour points of 0.1 mass% and 0.5 mass% nanolubricants were decreased. At the same time, it increased by 3.7% at 0.2 mass% nanolubricants compared with the other two samples.

The researcher found that the nanolubricant concentration (wt %) was the only driving factor in the pour point study; specifically, the 0.2 mass% was more influential in the increase in the pour point. To be specific, carbon-based nanostructures saw more improvement compared to copper oxide nanoparticles due to having most non-polar functional group.

## Stability

The main factor that affects the nature of nanolubricants is stability. According to the researchers, if stability decreases; a reduction is observed in all other properties of nanolubricants. Stability is a critical aspect of nanolubricants because of the tendency of agglomeration between nanoparticles is predominant, due to high surface energy of nanoparticles. According to Derjaguin, Landau, Verway, and Overbeek (DLVO) theory, Vander Waals force (attractive force) and an electrical double layer force (repulsive force) are the two forces between the nanoparticles. If the repulsive force is much higher than the attractive force, the nanolubricant is in a relatively stable state, as it overcomes the attraction because of collision due to Brownian movement. Otherwise, the nanolubricant is in an unstable state [70, 76, 144].

Steric repulsion and electrostatic repulsion are the other two types of mechanisms through which the nanolubricants gets stabilized as shown in Fig. 16. According to steric repulsion of several surfactants, such as SDS, SDBS, and CTAB can prevent the agglomeration of blended nanoparticles in nanolubricants. These surfactants usually have two tails; hydrophilic and lipophilic (hydrophobic). The hydrophilic tail adsorbs onto the surface of nanoparticles with a long loop, and the lipophilic tail extends out into the lubricants. Thus, stabilization of nanolubricants due to steric repulsion is well-dispersed and can sustain for an extended period. In electrostatic stabilization, all the nanoparticles in the fluid (polar) adsorb one type of ions on its surface through various mechanisms. So, an electrical double layer is created around each nanoparticle which offsets the attractive force between them [70, 76, 144]. The two stability mechanisms are depicted diagrammatically in Fig. 16.

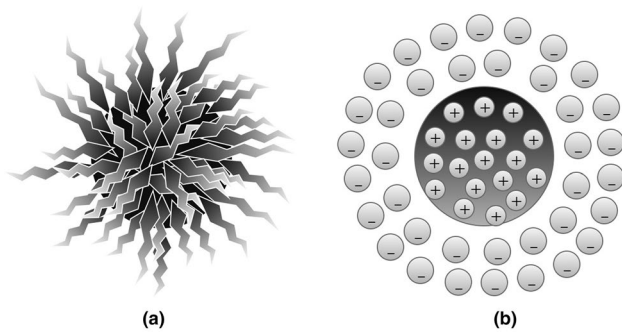


**Fig. 16** **a** Steric stabilization, **b** electrostatic stabilization

The selection of suitable surfactant is one of the key issues during stabilization of nanolubricants. The surfactants generally consist of a lipophilic tail portion; a long-chain hydrocarbon, and a hydrophilic polar head group. Surfactants are generally employed to increase the contact between two materials, sometimes known as wettability. In a two-phase system, a surfactant tends to introduce a degree of continuity between the nanoparticles and lubricants at the interface [70, 144]. Basically, the surfactants are classified into four classes (Table 4).

For nonionic surfactants, if the hydrophilic/lipophilic balance (HLB) is lower; it indicates that it is an oil soluble surfactants; on the other hand, if the HLB value is higher, it is a water-soluble surfactants. The HLB value is readily available in many handbooks [70, 145].

In general, it can be understood that when the base fluid of nano-colloids is a polar solvent, water-soluble surfactants are preferred as the polar functional group of surfactants adsorb nanoparticles in polar fluids. In this method, the hydrophilic

(water loving) surfactant adsorbs nanoparticles which create a bond with the polar fluids and thereby increasing the stability. On the other hand, oil being non-polar fluid, a non-polar functional group of surfactant adsorbs nanoparticles in non-polar fluids. In this method, the lipophilic (oil loving) surfactant adsorbs nanoparticles which create a bond with the lubricants, thereby increasing the stability [146]. The research on increasing the stability of nanolubricants is still under study [70, 144, 145].

Thus, the addition of surfactant is an effective way to enhance the stability of nanolubricants. The surfactants create a bond between nanoparticles and base lubricants. However, it is used to decrease the surface tension of base lubricants and improve the dispersion of nanoparticles. Although it has many merits, it is said that surfactants also cause several problems such as the addition of surfactants may damage the heat transfer media and may produce foams when heating process is carried out in heat exchange systems. Furthermore, the surfactant molecules bonded on the nanoparticle surface may enlarge the thermal resistance between the nanoparticles and base lubricant and hence it may limit the enhancement of the effective thermal conductivity [70, 144]. But the addition of surfactants also increases the viscosity of nanofluids which in turn enhances the tribological property of lubricant oil. At the same time, high viscosity of nanolubricants affects the lubricity. As a result, low amount of nanoparticles enters tribo-pairs when surfactant is added which ultimately decreases the tribological property of the nanolubricant. Additionally, surfactants are usually sensitive to temperature. At high temperature, surfactants could decompose and thus stay out of action [70, 76].

Table 5 shows that more number of research studies used different surfactants. To be specific, the oleic acid

**Table 4** Four classes of surfactants

Surfactants	Charge	Examples
Nonionic	No charge	Polyethylene oxide Poly ether Alcohols and other polar groups
Anionic	Negative	Carboxylate Sulfosuccinates Sulfates Phosphates Sulfonates
Cationic	Positive	Protonated long-chain amines Quaternary ammonium compounds
Amphoteric (or) zwitterionic	Negative and positive	Positive charge is almost ammonium Negative charge is both carboxylate ion and ammonium ion Carboxylate is by far the most common

surfactant-based research works are observed more in number. Similarly, the SDS and Span-80 surfactant-based literatures are also prevalent. At the same time, some of the research works are also investigated without the usage of surfactants.

Details of the stability study of nanolubricants reported in literatures are furnished in Table 9 (refer in Appendix 3).

## Stability analysis method

Figure 17a displays the different stability analysis used in the previous literature. The researchers used stability methods such as visual analysis, DLS, UV, zeta potential, centrifugation method, refractometer, and TEM imaging [70, 76, 144, 150–152]. However, the most widely used method was visual observation method or sedimentation method. It is best suitable in nanolubricant stability analysis than other methods. The other methods are DLS, UV, TEM, and zeta potential. The reason is generally because of the absorbance nature of nanolubricant is less or possesses a medium

transparency which drives us to study using visual observation method or sedimentation method.

## Sedimentation (or) photograph capturing method

Sedimentation method is the simplest method to analyze the stability of nanolubricants. Sedimentation of the nanoparticles is observed through a transparent glass container, in which nanolubricant is filled, and photographs are taken [70, 76, 144, 150–152].

Kumar et al. [5] analyzed the stability of Cu–Zn-based nanolubricant at 0, 0.1, 0.3, and 0.5 mass% concentration in three different base lubricants (vegetable oil, paraffin oil, and SAE oil). The stability was tested every day without any disturbances. The stability results indicated that all samples were stable till 72 h and then nanoparticles started to agglomerate. After 168 h, almost all nanoparticles settled down. They concluded that SAE oil-based nanolubricant had less agglomeration than vegetable oil and paraffin-based nanolubricants.

Pena-Paras et al. [13] studied the stability of copper oxide, alumina/oleic acid-dispersed poly-alpha-olefin (PAO8) oil,

**Table 5** Surfactants used in pervious literatures

Surfactant	References
SDS	[5, 23, 44, 54, 61, 128]
Oleylamine	[6, 104, 129]
Oleic acid	[8, 9, 17, 18, 27, 30, 31, 82, 83, 90, 104, 109, 121, 131, 147]
KH-560	[11, 12, 15]
Estisol and Pluronic	[129]
Span-80	[21, 46–48, 88, 118]
Sodium oleate	[24]
Dodecylamine	[36, 42, 95]
PVP	[41, 124]
CH-5	[45]
Poly-isobutylene	[52]
Aliquat 336	[56]
Tween- 20	[57]
vinyl methylerichlorosilane/methyl methacrylate	[59]
Triethanolaminemonooleate	[122]
Glycol	[101]
Hyper-dispersant produced in three source surfactants (maleic anhydride, oleic acid, styrene, 2,2'-azobisiso-butyronitrile)	[131]
Span-60 (Sorbitanmonoostreate)	[108, 123]
Tributyl phosphate	[117]
Poly ethylene glycol - 2000	[120]
Alkyl aryl sulfonate	[106]
CTAB	[107]
Diocylaminedithiocarbamate	[99]
ZDDP	[114]
Gum Arabic	[97]

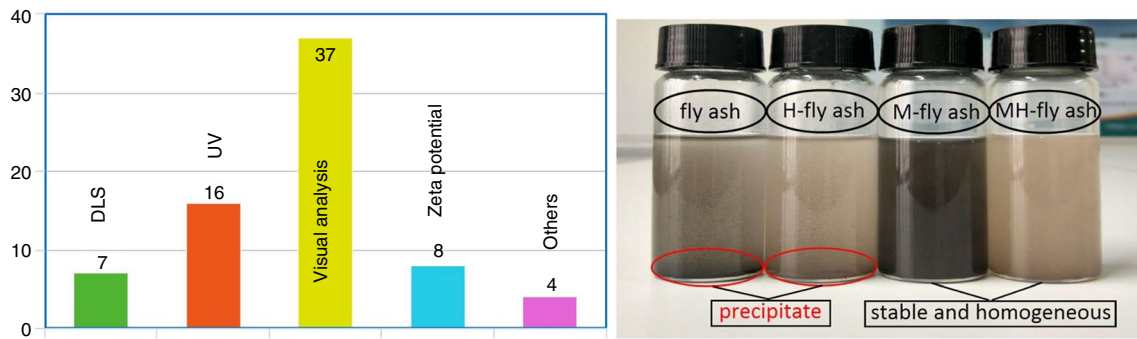


Fig. 17 a Stability methods used; b visual analysis of PAO with addition of four types of lubricant additives after storage for 168 h [90]

Fig. 18 a TEM image of 10 mass% Ag–MoS<sub>2</sub> deposited on worn surface, b electron diffraction patterns of TEM image, c EDX analysis of Ag–MoS<sub>2</sub> elements presents on worn surface

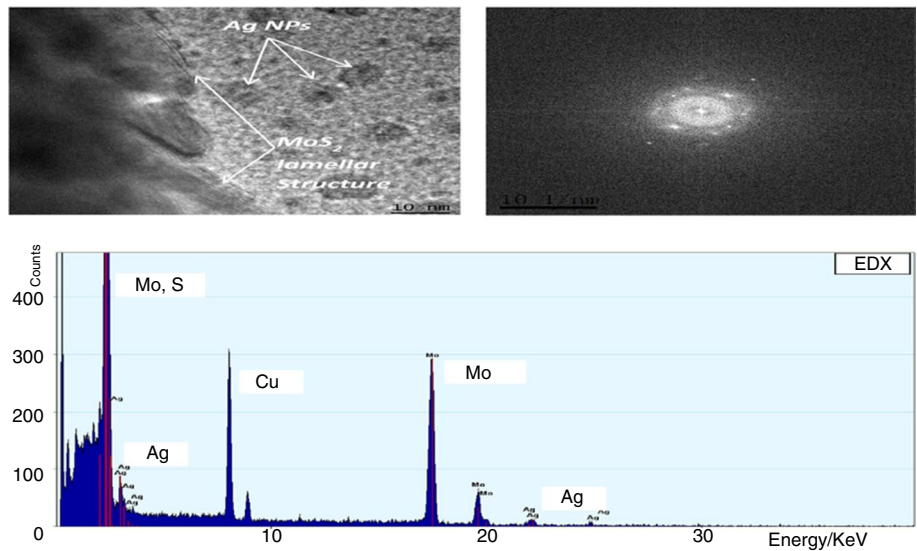
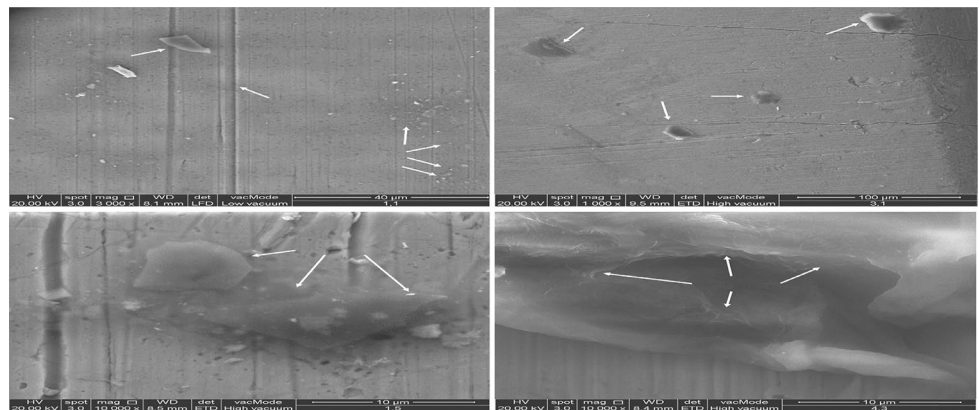


Fig. 19 SEM images of graphene nano-flaks on worn surfaces is sliding (left-top), folded (right-top), buckled (left-bottom), warped (right-bottom)



and the nanolubricant showed better stability after using oleic acid. Luo et al. [15] studied the stability of KH-560-modified spherical structure Al<sub>2</sub>O<sub>3</sub>/TiO<sub>2</sub>-based nanolubricant and found that the prepared nanolubricants showed excellent stability. Ingole et al. [29] studied the stability of nano-sized TiO<sub>2</sub> (anatase) and commercially available TiO<sub>2</sub>

(rutile)-dispersed mineral oil without any surfactant. The results showed that the stability of TiO<sub>2</sub> (anatase) nanolubricant was better than TiO<sub>2</sub> (rutile) nanolubricant.

Li et al. [21] tested the stability of GN<sub>5</sub>-Cu composite nanoparticles dispersed in lubricating oil/span-80 (0.2 mass%) composition, and its stability was observed

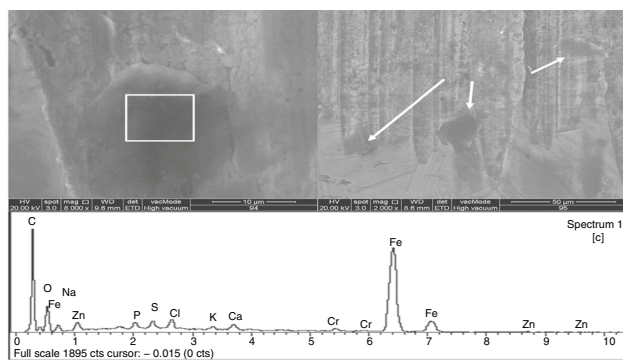


**Fig. 20** Graphene flakes stuck in worn surface due to natural polymeric ester-based lubricant additive (top left and right), (C)–corresponding EDX of graphene

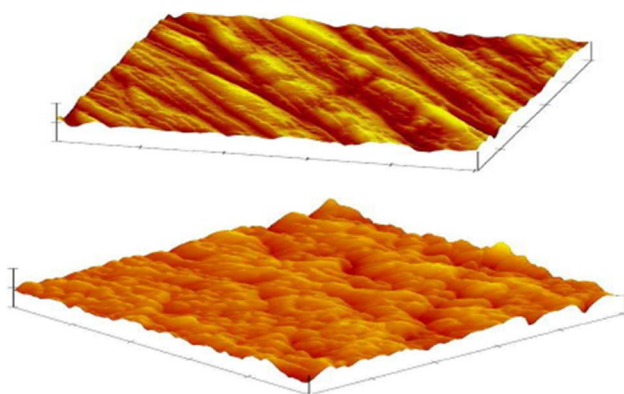


**Fig. 21** (Top) Liquid paraffin (Bottom) Liquid paraffin + 0.2 mass% SiO<sub>2</sub> particles

after 20 days. The dispersion of nanolubricant was observed to be stable with slight sedimentation. They also analyzed the UV absorbance of the sample and found that absorbance decreased slowly with increase in time. Lee et al. [37] examined the stability of various nanoparticles (C<sub>60</sub>, MWCNTs, CuO)-dispersed mineral oil. The results showed that the C<sub>60</sub>-based mineral oil was stable for about 800 h after preparation and maintained the dispersion over 80%. The MWCNTs nanoparticles were found to be 70% sediment in mineral oil within a span of 50 h, and 40% of CuO nanoparticles were also sediment in mineral oil in 500 h. Thus, they concluded that the MWCNTs and CuO-based nanolubricants have poor stability.

Zhang et al. [47] investigated the stability of span-80/diesel soot/graphite nanoparticles-based lubricating oil. 1 mass% of Span-80 added lubricating oil was found to be stable and the stability reduced after 72 h. Viesca et al. [26] carried out the stability of carbon-coated copper nanoparticles and non-carbon-coated copper nanoparticles dispersed in PAO base oil. Both samples had better stability at the

end of friction testing. Xie et al. [80] investigated the stability of nano-sized SiO<sub>2</sub> and MoS<sub>2</sub> particle-based lubricating oil. The SiO<sub>2</sub>-dispersed lubricant showed excellent stability. On the other hand, the MoS<sub>2</sub> dispersed samples tended to agglomerate due to their poor dispersion in the base lubricant.

Peng et al. [83] investigated the stability of modified and unmodified SiO<sub>2</sub> nanoparticles/paraffin oil. The modified SiO<sub>2</sub> nanoparticles were stable in paraffin oil and hardly any sedimentation of particles was observed. However, the unmodified SiO<sub>2</sub> nanoparticles aggregated and precipitated within few hours. Hence, the oleic acid modification of nanoparticle was an effective way to improve the stability.

Gulzar et al. [84] determined the stability of TiO<sub>2</sub>/SiO<sub>2</sub> nano-composite-based nanolubricants used at different concentrations (0.25 mass%, 0.50 mass%, 0.75 mass%, and 1 mass%). They reported that 0.75 mass% of TiO<sub>2</sub>/SiO<sub>2</sub> nanolubricants showed appreciable stability. Guo et al. [88] investigated the stability of three type of heavy vehicles diesel soot (A, B, and C)/span-80-based nanolubricants. They selected common concentration of diesel soot such as PAO 4 + 0.05 mass% soot + 1 mass% SP. Finally, it was observed that PAO 4 + 0.05 mass% soot A + 1 mass% SP (soot A) had higher stability compared to other diesel soots.

Gao and Luo [131] investigated the stability of Cu/hyper-dispersant-based nanolubricants. The result showed that this combination of nanolubricant was stable around 21 days of preparation. The dispersion stability improvement of ultrafine inorganic particles was noticeable; because the nanoparticle surfaces absorb the hyper-dispersant. The polymer chains capped on the surface of nanoparticles, prevented aggregation and increased the stability. Due to capping, the nano-Cu surface was transformed from hydrophilic to hydrophobic nature. The stable dispersion of modified nanoparticles added nanolubricants was due to the steric repulsion among polymer chains. The surface of inorganic nanoparticles coated with an organic layer could reduce the interface energy of nanoparticles and decrease the interaction between the nanoparticles and prevent the agglomeration.

Cao and Xia [90] examined the stability of various fly ash-based nanolubricants. The fly ash materials such as fly ash, OA-modified fly ash (M-fly ash), treated fly ash (H-fly ash), and OA-modified treated fly ash (MH-fly ash) were used. The results proved that the M-fly ash and MH-fly ash-based nanolubricant sample provided effective stability compared with fly ash and treated fly ash nanolubricant sample.

Kotia et al. [96] evaluated the stability of Al<sub>2</sub>O<sub>3</sub> and SiO<sub>2</sub>-based nanolubricants at 0.3, 0.6, and 0.9% volume fraction. In this study, density of the nanoparticles was measured with varying sedimentation time. It can be observed that the higher volume fraction samples were maintained stable at above 95% compared to the initial volume fraction. They explained that it was due to the supernatant and

non-Newtonian behavior of nanolubricant. Lower volume fraction added nanolubricants was observed to be more stable. Moreover, it was predicted that agglomerated size of the SiO<sub>2</sub> nanoparticles was larger than agglomerated Al<sub>2</sub>O<sub>3</sub> nanoparticles.

### Dynamic light scattering (DLS) method

DLS is used for evaluating the stability of nanolubricant; the tendency of the nanoparticle to aggregate over time is taken as a control parameter. This instrument is used to measure the average particle size of the nanoparticle suspended in the lubricant sample with time. However, the nanoparticles in the fluid move randomly, and their speeds of movement is used for determining the size of the particle [5, 89, 151, 152].

Kumar et al. [5] investigated the stability of Cu–Zn nanoparticles (0.1, 0.3, 0.5 mass%) in three different base lubricants (vegetable oil, paraffin oil, and SAE oil) and its size distribution change due to natural sedimentation by measuring the samples every day. Their results indicated that the all samples were stable till 72 h and then agglomeration of particles started and almost all the particles tended to settle down.

Ali et al. [9] investigated the stability of Al<sub>2</sub>O<sub>3</sub> and TiO<sub>2</sub> nanolubricants. The dynamic light scattering (DLS) peak diameter of Al<sub>2</sub>O<sub>3</sub> (43.82 nm) and TiO<sub>2</sub> (24.36 nm) nanoparticles was more significant than the primary size of single nanoparticle of Al<sub>2</sub>O<sub>3</sub> = 8–12 nm and TiO<sub>2</sub> = 10 nm. This change was due to slight agglomeration of the nanoparticles in the engine oil due to strong Vander Wall interactions (intermolecular forces). The Al<sub>2</sub>O<sub>3</sub> and TiO<sub>2</sub> nanoparticle sizes increased with time due to sedimentation, but it did not form large clusters, and it was stable over the time of about 336 h (14 days) at room temperature. However, the stability was not better with increase in the storage time because of aggregation of the nanoparticles which was evident by the increase in the DLS peak diameter. The aggregation occurred whenever the Brownian motion and the attractive forces (Vander Wall) of the nanoparticles were greater than the repulsive forces.

Zin et al. [39] studied the stability of CNHs nanolubricants using DLS method. The DLS test was conducted for 2 weeks, and it confirmed the static dispersion of all (0.1, 0.2, 0.5 and 1 mass%) samples. However, the 1 mass% of nanolubricant sample was not tested due to its high viscosity (do not passing the laser light on dark area). The measured average diameter of nanoparticles did not change significantly during the measuring time, lead to assume that there were no aggregation phenomena. The study reported that the mean aggregate size measured for all mass% of CNHs, and its percentage deviation was below 10% for all suspensions.

Moreover, they mentioned that no sedimentation occurred and thus confirming an excellent stability.

Zin et al. [41] studied the stability of Cu<sub>1</sub>, Cu<sub>2</sub>, TiO<sub>2</sub>, and SWCNHs (0.005, 0.01, 0.02 vol%)-based nanolubricants. The test was carried out for 2 weeks, and the stability was acceptable for all suspensions over the span of testing time of various mean sizes and structure of nanoparticles. However, they said that there was no significant variation of suspended nanoparticle aggregates detected over time period.

Srinivas et al. [52] carried out the stability study of MoS<sub>2</sub> (0.25, 0.5, 0.75 and 1 mass%)-based nanolubricant. The 0.5 and 1 mass% of nanolubricant stability was analyzed after 10 days of preparation. The results showed that 0.5 mass% MoS<sub>2</sub>-based nanolubricant displayed effective stability. At the same time, the 1 mass% of MoS<sub>2</sub> nanolubricant had poor stability due to agglomeration of nanoparticles forming large clusters. Therefore, they suggested 0.25 to 0.5 mass% of MoS<sub>2</sub> for good stability.

Lineira del Rio et al. [91] checked the stability of TMPTO/PAO/rGO-based nanolubricants using dynamic light scattering method. They observed apparent (agglomerate) average size of dispersed graphene nanosheets for both base oils. The apparent sizes of TMPTO and PAO 40 nanolubricants were around 630 nm and 60 nm, respectively. This study used the concentration 0.25 mass% (rGO) for both base oils. The minimum apparent average size was obtained for PAO 40/rGO nano-dispersion, and it may be due to lesser possibility of collision of the nanoparticles in highly viscous lubricants (lower Brownian motion). The DLS data revealed that both nanolubricants did not sediment for 70 h after sonication.

### Zeta potential method

Zeta potential is the electric potential in liquid layer surrounding the particles containing two different regions; an inner region (stern layer) and an outer (diffuse) region. At the inner region, ions are firmly bound and are loosely associated at the outer region. The value of zeta potential is a measure of the stability of solid in liquid mixtures. So, solid/liquid mixtures with high zeta potential (negative or positive) are electrically stabilized, while the mixtures with low zeta potentials values tend to coagulate or flocculate. In general, a value of 25 mV (positive or negative) can be taken as an arbitrary value that separates minimum-charged surfaces to maximum charged surfaces. The mixtures with zeta potential from 40 to 60 mV are believed to possess good stability, and those with more than 60 mV have excellent stability [70, 76, 144, 150–152]. At the same time, very less value (ex: –1.72 mV and –0.516 mV) indicates electronegativity (non-conducting) characteristic-based nanolubricants, but they not said this value considers for stability [47, 88].

Luo et al. [11] examined the stability of KH-560-modified  $\text{Al}_2\text{O}_3$  nanolubricants. The absolute zeta potential value of modified  $\text{Al}_2\text{O}_3$  nanolubricants was 25.1 mV, which was greater than the value of unmodified  $\text{Al}_2\text{O}_3$  nanolubricants; it indicates the static repulsion of modified  $\text{Al}_2\text{O}_3$  nanoparticles is higher than unmodified  $\text{Al}_2\text{O}_3$  nanoparticles. They reported that modified  $\text{Al}_2\text{O}_3$  offered more resistance to agglomeration and sedimentation in lubricating oil.

Vattikuti and Byon [53] investigated the stability of nano-flowers and nano-sheets structured  $\text{MoS}_2$  nanolubricant. They found that 0.1 mass% of  $\text{MoS}_2$  nanosheet-based nanolubricant had better stability compared to base lubricant. The absolute value of zeta potential was higher than 30 mV; thus, the nanolubricant was stable. The study suggested both nanolubricants had absolute zeta potential value of 32 and 34 mV, respectively, and it was an indication of good stability. They denoted that dispersive nature of the nanolubricants depended on parameters like concentration (Mass percentage of nanoparticles), nature of the base lubricant, and temperature.

### Spectral absorbency method

Spectral absorbency method is another efficient way to evaluate the stability of nanolubricants, but the UV absorbance study of nanolubricant was very limited. Passing absorbance spectrum through a nanolubricant filled cuvette is not an easy task because the spectrum can pass only through transparent colloids. Thus, lesser concentration nanolubricants are generally most suitable for UV absorbance study. In general, there is a linear relationship between the absorbency intensity and the concentration of nanoparticles in oil. Normally, nanomaterials dispersed in lubricants or fluids have characteristic absorption bands in the wavelength of 190–1100 nm. The variation of dispersed nanoparticle sedimentation in nanolubricants can be obtained by the measurement of absorption of nanolubricants because there is a linear relationship between the absorption spectrum and amount of suspended particles [4, 70, 109, 150–152].

Ali et al. [9] analyzed the stability of oleic acid-modified  $\text{Al}_2\text{O}_3$  and  $\text{TiO}_2$  nanolubricants. The spectrum peak of maximum wavelength ( $\lambda_{\text{max}}$ ) of the OA-modified  $\text{TiO}_2$  and  $\text{Al}_2\text{O}_3$  nanolubricant was 490 and 482 nm, respectively. At the same time, the peak wavelength of lubricant containing OA was 470 nm. They mentioned that it was lower than other samples. The higher peak of absorbance suggests a better suspension of nanoparticles in engine oil. Also, oleic acid-modified  $\text{TiO}_2$  nanolubricant showed effective dispersion than oleic acid-modified  $\text{Al}_2\text{O}_3$  nanolubricants.

Thottackkad et al. [18] conducted the stability study of surfactant with CuO/coconut oil-based nanolubricants. At the end of the research, the surfactant-added nanolubricant exhibited excellent stability.

Peng et al. [31] studied the stability of oleic acid-modified diamond and  $\text{SiO}_2$ /paraffin oil-based nanolubricants and evaluated the stability by UV spectrum-photometry method. The stability results of modified nanoparticles/liquid paraffin showed that the absorbance spectrums slightly increased with time, so it indicated better stability. The  $\text{SiO}_2$  nanolubricants absorbance value was higher than diamond nanolubricants. The researcher pointed out the  $\text{SiO}_2$  nanoparticles did not sediment easily due to its low density and higher surface area. Finally, the study suggested, modified nanoparticles using oleic acid is an effective way to improve stability of nanolubricants. And the oleic acid surface-modified layer effectively prevents the agglomeration of nanoparticles.

Huang et al. [46] studied the stability of span 80 modified graphite nanolubricants. The Span-80 surfactant-modified graphite nanosheets was prepared using ball milling process, and then the prepared modified nanoparticles were blended in paraffin oil. Then, these colloids were dried under heat, and then the dried combination of span-80/paraffin oil-modified graphite nanosheets was dispersed on pure paraffin oil. Finally, the results confirmed that 1 mass% of span 80 with paraffin oil-modified graphite nanosheet-based nanolubricants showed excellent stability.

Koshy et al. [54] studied the stability of SDS-modified  $\text{MoS}_2$  nanolubricants. The prepared samples were kept idle for a span of 100 days after sonication. This study stated that surfactant-modified  $\text{MoS}_2$  nanoparticles dispersed lubricants had limited traces of sedimentation even after 100 days exhibiting excellent stability.

Thottackkad et al. [57] studied the stability of OA-modified  $\text{CeO}_2$  nanoparticle blended with various base lubricants (coconut oil, paraffin oil, and SAE15W40 oil). The results showed that the non-modified nanoparticles blended lubricants' settling trend was stable after long period of the storage. However, the surfactant-modified nanoparticles blended lubricant settling trend was reduced due to certain extent of formation of micelle-like structure.

Jatti and Singh [79] evaluated the stability of mineral oil-based CuO nanolubricants. They claimed that CuO nanoparticle showed good stability in mineral oil, which was confirmed by UV-spectra photometer.

Gulzar et al. [84] investigated the stability of  $\text{TiO}_2$  and  $\text{TiO}_2/\text{SiO}_2$  nanolubricants. The stability increased for the nanoparticle concentration of 0.25–0.75 mass% for both type of nanolubricants. The enriched nano- $\text{TiO}_2$  suspensions showed less stability as the separation interfaces between the sediment and the supernatant were sharp after being initially stable for a few hours which then gradually declined with time. A clear lubricant was visible after 3 days because the enriched nano- $\text{TiO}_2$  particles were subjected to continuous sedimentation and separation. On the other hand, there was a stable dispersion of nanoparticles even in the absence of a surfactant in  $\text{TiO}_2/\text{SiO}_2$  nano-composite. Specifically,



0.75 mass% nano-TiO<sub>2</sub>/SiO<sub>2</sub> nanoparticles provided effective stability. However, they claimed that this stability depended on concentration because for a further increase in concentration to 1 mass% of TiO<sub>2</sub>/SiO<sub>2</sub> nano-composite observed an absorbance curve drop rapidly after 24 h as the particles started to agglomerate more. Furthermore, 1 mass% nano-TiO<sub>2</sub>/SiO<sub>2</sub> enriched composite was exhibiting higher rate of deposition after 3 days.

Song et al. [109] studied the stability of OA-modified ZnAl<sub>2</sub>O<sub>4</sub> nanoparticle-based lubricant at the concentrations of 0.05, 0.1, 0.5, and 1 mass% at temperatures of 30 °C, 70 °C, and 110 °C, respectively. The dispersion rate was low at the temperature of 30 °C and 110 °C. However, better dispersion was achieved for 0.5 mass% at 70 °C. Then, they compared the stability of various concentration of oleic acid modifier addition (3, 6, 9, and 12 mass%) in ZnAl<sub>2</sub>O<sub>4</sub> nanolubricants. The results showed that better stability was observed between concentration from 3 to 9 mass%. Moreover, the 12 mass% modifier samples showed similar results to the dispersion of 9 mass% modifier sample. They said that the modifier concentration and heating temperature are both important for improving the dispersion stability of nanolubricant.

Hwang et al. [153] studied the stability of various nanoparticles such as MWCNTs, C<sub>60</sub>, copper oxide, silicon dioxide, and silver in the nanolubricant using UV-spectra method. The stability study of fullerene nanoparticle confirmed that the particles were well-dispersed in base lubricating oil due to its exquisite nature. However, the MWCNTs mixed lubricating oil sample had poor stability due to its fashionable structure and complexity.

Alves et al. [93] examined the dispersion of CuO nanoparticles in the lubricant using UV absorption spectroscopy. Generally, higher absorbance value indicates better dispersive nature of the nanoparticles in lubricant. They found the absorbance values of wavelength of about 240–300 nm for the CuO nanoparticle. The highest absorbance peak of the CuO in oil solution with 0.1% of concentration was at a wavelength of 270 nm. This highest absorbance and unique peak of wavelength of 250 nm indicate good dispersion of CuO nanoparticles in lubricant oil. As the nanolubricants with 0.25 and 0.50 mass% were dark, it was necessary to dilute. And the spectra of diluted solutions were also similar to 0.1 mass% CuO nanoparticle. Better dispersion was achieved by superficial modification using oleic acid and dispersant agent namely Toluene.

## Other methods

### TEM imaging method

Generally, it is used for characterizing the morphology (3D) of nanoparticles before dispersion. The transmission electron

microscopy (TEM) provides high-resolution images that can reach approximately 0.1 nm in case of lattice images. The aggregation of nanoparticles within the nanolubricants can be directly monitored with TEM imaging [76, 150–152].

Zawawi et al. [14] studied the stability of the Al<sub>2</sub>O<sub>3</sub>–SiO<sub>2</sub>/PAG-based nanolubricants using TEM imaging technique; TEM image was used to observe the dispersion and stability of hybrid nanolubricants at 88,000X magnification. The results showed that highest concentration (1 mass%) ratio with optimum sonication time represents the most stable nanolubricant. It should be noted that there was no surfactant used in this study. The usual practice of characterization of nanoparticles dispersed in lubricant with TEM is by first placing a drop of prepared nanofluids onto a copper grid coated with a carbon film. Then, the grid is observed for the distribution of nanoparticles on copper grid when base lubricant completely dries [76].

### Centrifugation method

The centrifugation method is also used to analyze the stability of nanolubricants. The centrifuge instrument is based on the principle of centrifugal force on nanolubricants under various speed (in rpm) and time (in minutes). Finally, the nanolubricant is visually checked for any sediment in the transparent glass container [151, 152].

Liu et al. [58] analyzed the stability of surface-modified composite of rare earth naphthenate nanoparticles dispersed in commercially available solvents such as VG (Virgin 26) white oil, toluene, benzene, and petroleum ether. The study found that the 15 mass% of nanoparticles mixed solvent showed excellent stability at –10 °C.

Shaharuddin et al. [148] determined the stability of graphene nanolubricants by centrifuge method. This method of stability test was used in this experiment to confirm the results in a short period of time. The centrifugal device (Scan Speed 1730RPM) was used where all the samples of a total of 12 were put into the device for 10 min. The four sets of nanolubricants samples were tested for four different rotational speeds—1000 rpm, 5000 rpm, 10,000 rpm, and 15,000 rpm. Then, the photograph taken before and after was compared. They noted that no sediments were observed after the centrifugal test. This test confirmed that all the prepared nanolubricants were stable. In this study, no surfactant was added. According to DLVO theory, the nanolubricants are stable because of the adequately high repulsive force as compared to the attractive force. So, the nanolubricants are considered to be stable. This is also due to the hydrogen (H) bond interactions between the deep eutectic solvents and graphene oxide nanoparticles, owing to the presence of hydroxyl (OH) groups in glycerol and the unique structure of graphene oxide nanoparticles. It is known that graphene oxide NPs have many functionalized groups such as

carbonate, hydrogen, carboxyl, phenol, carbonyl, and ether that contribute to the susceptibility of the strong hydrogen bonds.

### Refractory index method

Lineira del rio et al. [91] prepared the rGO and GO-based nanolubricants at various concentrations (0.05, 0.10, 0.25, and 0.50 mass%) in the base lubricant, TMPTO or Polyalphaolefin 40. They selected 0.25 mass% for stability analysis because it was in the intermediate range of the nanolubricant preparation. The first symptom of sedimentation in the GO-based nanolubricants was observed on sonication after 24 h. At the same time, for rGO-based nanolubricants, no sedimentation was observed even after 240 h for both the base oils. Researchers further analyzed the stability of rGO/GO nanolubricants using refractometer method, and its result showed that the stability of rGO nanolubricant was better. The increase in the refractive index was lower for the nano-dispersions containing rGO than for those containing GO

regardless of both base oil. These results showed that great stability improvement was observed in the nanolubricant containing rGO than GO, because of GO had most of polar functional group compared to rGO nanosheets (non-polar). So, the GO (polar) mixed lubricants (non-polar) showed no appreciable stability for base lubricants TMPTO and PAO.

### Summary of the review

The forgoing discussion about the review on the effects of nanoparticles on the tribological and thermo-physical characteristics of base lubricants is summarized in Table 6.

### Scope for future research work

From this review, it is found that more number research works dealing with single nanomaterial-based nanolubricants are reported in literatures. But, hybrid nanoparticles

**Table 6** Summary of the current review

Tribological and thermo-physical properties	Remarks
Friction and wear	<p>Non-polar functional group contained hybrid and mono-nanoparticle-based nanolubricant showed higher friction and wear resistance property</p> <p>Oleic acid and oleylamine-based-modified nanostructures show synergistic effect of friction/wear reduction, due to increasing the antioxidant nature of nanolubricant</p> <p>Friction and wear reduction in non-polar (like metal, carbon)-based nanolubricants are higher than metal oxide-based nanolubricants due to increasing polar (Al–O, Ni–O, Ti–O, O–H) function group in nanolubricant</p> <p>Mostly low concentration with higher surface to volume ratio of nanoparticles shows better tribological effect</p> <p>Specifically, conducting, semiconducting, and insulating nature of carbon nanostructures shows excellent tribological properties due to non-polar nature</p>
Thermal conductivity	<p>Thermal conductivity of nanolubricants increases with increasing temperature</p> <p>Metal, metal oxide, carbon (conducting nanostructures) and hybrid nanoparticles having higher surface to volume ratio-based nanolubricant shows higher thermal conductivity</p> <p>Stable aggregation or distinct nanostructures with higher surface area show better thermal conduction mechanisms</p> <p>Thermal conductivity of nanolubricants increases due to uniform arrangement of nanoparticle aggregation with better suspension nature</p> <p>Large inter particle distance between the nanoparticles shows low thermal conductivity</p> <p>Thermal conductivity increases with concentration of nanoparticles but the increase in thermal conductivity has no direct relationship with other lubricant properties like friction/wear, kinematic viscosity, flash point and pour point</p>
Kinematic viscosity	<p>Stable aggregation or mono-nanoparticles help to enhance the lubricant viscosity</p> <p>Kinematic viscosity enhancement depends on working temperature and nanostructures concentration</p> <p>Specifically, non-polar functional group with better surface area contained nanoparticles helps to improve the viscosity index in base lubricant</p>
Flash point	<p>Flash point is higher for non-polar than polar nanoparticles</p> <p>Flash point increases with concentration of nanoparticles</p> <p>Higher the flash point of nanolubricant greater its thermal stability</p>
Pour point	<p>Non-polar (C–H, C=C=C, C=C, C≡C) functional group contained carbon nanostructures shows higher pour point</p>
Stability	<p>Nanolubricant with higher surface to volume ratio and optimum concentrations of nanoparticle exhibits excellent stability</p> <p>Oleic acid and oleylamine-based non-polar surfactant shows better stability in lubricant medium, due to reduced agglomeration (intermolecular forces) between the nanoparticles</p> <p>Specifically, carbon-based nanostructures showed better stability than other nanostructures due to similar functional group</p>

are highly suitable for the use in lubricant to conduct excess heat. There are only a few nanolubricant research studies involving nano-composite or hybrid nanomaterials have been carried out. Hybrid nanoparticles involving various combinations any two among metal, metal oxide, and carbon nanoparticles can be synthesized and its effect on tribological and thermo-physical properties could be studied. It should be noted that particularly, the nanoparticles should be having high surface to volume ratio.

Additionally, carbon nanostructures can be prepared by either chemical or natural method. Generally, the carbon-based nanostructures enhance both tribological and thermo-physical property of base lubricant to a greater extent than any other nanoparticles. The carbon and carbon-based nanostructures are most widely prepared by chemical methods due to its easy accessibility and availability even though it uses high toxic chemicals. Extraction of conventional carbon nanostructures like MWCNTs, graphene, and graphene oxide from various natural sources like coconut shell, green plant, etc., which would be economical and provide environmental safety, will have to be explored.

In stability additive point of view, although the use of surfactant enhances stability, it can both increase and decrease the nanolubricant property. Therefore, it is advisable to identify the suitable surfactants with amount (mass% or vol%) for corresponding nanolubricants before the nanolubricant is put to practical use.

## Conclusions

In this review article, the effect of adding mono- and hybrid nanoparticles on the tribological and thermo-physical properties of base lubricant is reviewed in detail and the influence of nanoparticle shape, size, material, and concentration, temperature, and surfactant are thoroughly analyzed and reported. More importantly, the enhancement in tribological and thermo-physical properties is dependent on the uniform and stable dispersion of nanoparticles in the base lubricant. The important points recorded from the review are listed below:

- The tribological properties such as friction and wear change is primarily based on factors like base lubricants, nature of nanoparticles, nanoparticle size, nanoparticle structure, working temperature, nanoparticle concentration, purity of nanoparticle, nanoparticle agglomeration, surfactants, nanolubricant stability, and preparation method.
- Increasing nanomaterial concentration in lubricants increases the tribological property which invariably increases up to a certain concentration and then decreases. Some specific concentrations are only suitable for improving the tribological performance of nanolubricants.

- Researchers confirmed that there are mainly four types of mechanism such as sliding, rolling, bearing, and tribofilm formation in reducing the friction with the aid of nanoparticles in the base lubricant. But, tribofilm formation mechanism is the major friction reduction mechanism as reported in many research studies in nanolubricants.
- The thermo-physical properties such as thermal conductivity, kinematic viscosity, and flash point increase or decrease based on various factors such as base lubricants, nature of nanomaterials, nanomaterials size, nanomaterials structure, working temperature, nanomaterials concentration, purity of nanomaterials, nanoparticle agglomeration surfactants, and nanolubricant stability.
- Specifically, 'carbon nanostructures' pour point increment was better than other nanoparticles like metal, metal oxide-based nanostructures due to the presence of more non-polar functional groups.
- Increasing nanoparticle concentration increases the thermo-physical properties gradually and then it reduces. Some specific nanoparticle concentrations are only suitable for improving the thermo-physical properties of the base lubricant.

Thus, increasing nanoparticle concentration in lubricants increases both tribological and thermo-physical properties invariably up to a certain concentration, and then both properties decrease. But, the optimum concentration may not be the same for the two properties.

- According to many researchers, the shape of nanoparticles is found to be influencing the tribological properties, whereas it has negligible effect on the thermo-physical properties of the nanolubricant.
- Sustaining the stability of nanoparticles in lubricant for an extended period of time is a challenging task because of the tendency of the nanoparticles to agglomerate and settle down depending upon nanoclusters density. However, optimum concentration with higher surface area to volume ratio of nanoparticles exhibits excellent stability in base lubricants.

Due to the enhancement of tribological and thermo-physical properties of the lubricants using nanoparticles, practical applications of nanolubricants in systems will pave way for extending the useful life of the components being lubricated, increasing the fuel/energy efficiency subsequently improving the fuel/energy economy, reducing global fuel/energy consumption with reliable performance and reducing the hazardous emissions thereby saving mother earth.

## Appendices

### Appendix 1

See Table 7.

**Table 7** Summary of tribological effects of nanostructures on frictional worn surfaces

Nanoparticle [References]	Structure	Results of tribological effects/mechanisms on friction surfaces
Ag–MoS <sub>2</sub> [4]	Lamellar	See Fig. 18 The Ag–MoS <sub>2</sub> nano-tribofilm formed on worn surfaces
Bi and Bi/Cu [7]	Spherical	Bi and Cu nanoparticles promote filling and sedimentation on the worn surfaces
Al <sub>2</sub> O <sub>3</sub> [11]	Spherical	The Al <sub>2</sub> O <sub>3</sub> Self-laminating protective nano-tribofilms are formed on friction surfaces
Al <sub>2</sub> O <sub>3</sub> /SiO <sub>2</sub> [12]	Nearly spherical	Rolling mechanism formed the Al <sub>2</sub> O <sub>3</sub> /SiO <sub>2</sub> tribofilms on worn surfaces
CuO and Al <sub>2</sub> O <sub>3</sub> [13]	Spherical and tubular	Rolling effect of CuO/Al <sub>2</sub> O <sub>3</sub> nanoparticles on specimen worn surfaces
Al <sub>2</sub> O <sub>3</sub> /TiO <sub>2</sub> [15]	Spherical	Formation of Al <sub>2</sub> O <sub>3</sub> /TiO <sub>2</sub> nano-protective film on worn surfaces
TiO <sub>2</sub> [29]	Irregular	Formation of uniform TiO <sub>2</sub> nano-tribofilm on sliding surfaces
Cu and CuO [17]	Nano-rhombic and nano-rods	Rolling effect of Cu/CuO nanoparticles on worn surfaces
surface-coated natural serpentine [20]	Lamellar	Surface-modified natural serpentine nano-tribofilms formed on worn surfaces
Graphene-copper [21]	Rippled and Spherical	Graphene–copper nano-composite film was promoting Self-repair effects on damaged parts and surfaces
CuO [22]	Spherical	Third body and tribo-sinterization effect of nano-CuO particles on worn surfaces
CuO [24]	Quasi spherical	Rolling and mending effect of CuO nanoparticles on friction surfaces
CuO and ZnO [10]	Nearly spherical	Formation of CuO–ZnO nano-tribofilm on wear surfaces
CuO, ZnO and ZrO <sub>2</sub> [28]	Nearly spherical	Tribo-sintering effect of CuO, ZnO and ZrO <sub>2</sub> nanoparticles on wear surfaces
Diamond and SiO <sub>2</sub> [31]	Irregular	Formation of SiO <sub>2</sub> tribofilm on worn surfaces
Fe <sub>3</sub> O <sub>4</sub> [32]	Nano-flake	Self-repair effect of Fe <sub>3</sub> O <sub>4</sub> Nano-flakes on worn surfaces
Mn <sub>0.78</sub> Zn <sub>0.22</sub> Fe <sub>2</sub> O <sub>4</sub> [33]	Quite uniform	Formation of amorphous nano-composite tribofilms on worn surfaces
Fullerene(C <sub>60</sub> ) [37]	–	Polishing effect of fullerene nanostructures on worn surfaces
Tiny graphene [39]	Nano-horn	Tiny graphene Nano-horns by rolling/sliding mechanisms on frictional surfaces
Graphene [40]	Nano-flake	See Figs. 19 and 20
Graphene [72]	Nano-flake	Graphene preparation via solar radiation, it acted as Nano-bearing effect on wear surfaces
Graphene [73]	Platelet	Graphene act as the ball-bearing effect on specimen worn surfaces
Single-Walled Carbon nano-horn, CuO, TiO <sub>2</sub> [41]	Nano-horn, Dahlia spherical and Spherical	Sliding into rolling effect on the worn surfaces
Diesel soot and graphite [47]	Nearly spherical and Quasi circular	Sliding/rolling effects on the frictional surfaces
rGO-Cu [48]	Nanosheets Nearly spherical	Formation of rGO-Cu nano-composite tribofilms on friction surfaces
Rhenium-doped fullerene-like MoS <sub>2</sub> [49]	Platelet	Filling of rare earth composite nanoparticle on worn surfaces
Hexagonal-BN [51]	Lamellar	H-BN Protective layer formed on the worn surfaces

**Table 7** (continued)

Nanoparticle [References]	Structure	Results of tribological effects/mechanisms on friction surfaces
MoS <sub>2</sub> [52]	Hexagonal	MoS <sub>2</sub> protective layer formed on the worn surfaces
MoS <sub>2</sub> [54]	Lamellar	Formation of MoS <sub>2</sub> nano-tribofilm on contact surfaces
CeO <sub>2</sub> [57]	–	Rolling effect of CeO <sub>2</sub> nanoparticles on sliding surfaces
Surface-modified nano-Y <sub>2</sub> O <sub>3</sub> [59]	Spherical	Formation of ceramic nano-protective layer on wear surfaces
Nickel [78]	Nearly spherical	Formation of Nickel nano-protective layer on the worn surface (tribo-sinterisation effect)
CuO [79]	Nearly spherical	Deposition of CuO nano-tribofilm on worn surfaces
MoS <sub>2</sub> and SiO <sub>2</sub> [80]	Nanosheets and Spherical	Rolling effect of MoS <sub>2</sub> and SiO <sub>2</sub> on wear surfaces
Cu [81]	Oblong	Formation of Cu metal nano-protective film on worn surface
Nickel [82]	Spherical	Deposition of Nickel nano-lubrication film on worn surfaces
SiO <sub>2</sub> [83]	Spherical	See Fig. 21 Formation of SiO <sub>2</sub> nano-protective film on worn surfaces
Diamond [85]	Slice	Formation of diamond protective layer on worn surface
MoS <sub>2</sub> [86]	Nanotube	Formation of wear protective layer and low-shear-tribofilm on worn surfaces
Diesel soot(3 types) [88]	Spherical and Elliptical	Sliding/rolling effects of diesel soot on the frictional surfaces
2D-Boron nitride [89]	Nano-platelet	Formation of 2D-Boron nano-tribofilm on worn surfaces
CaCO <sub>3</sub> [78]	Nearly spherical	Formation of CaCO <sub>3</sub> nano-protective film on contact surfaces
CuO, TiO <sub>2</sub> , and Nano-Diamond [101]	Spherical	Rolling effect on the sliding surface
Graphene [125]	Platelets	Formation of graphene nano-tribofilm on worn surfaces
Graphene [102]	Sheet	Formation of graphene nano-tribofilm on worn surfaces
La(OH) <sub>3</sub> -RGO [112]	Rod and sheet	Formation of Graphene and MoS <sub>2</sub> nano-tribofilm on worn surfaces
Lanthanum tri-fluoride [117]	Hexagonal	Formation of lanthanum tri-fluoride nano-tribofilm on rubbed steel surfaces
Serpentine/magnesium hexasilicate [103]	Irregular sphere and column	Self-repairing effect of serpentine/magnesium nano-tribofilm on worn surfaces
Carbon [113]	Nano-capsule	Carbon act as rolling effect on friction surfaces
Si <sub>3</sub> N <sub>4</sub> /SiC [119]	–	Rolling effect of Si <sub>3</sub> N <sub>4</sub> /SiC nano-tribofilm on frictional surfaces
Ni [128]	Spherical	Formation of Nickel tribofilm on worn surfaces
Cu [120]	Spherical	Formation of Cu nano-tribofilm on worn surfaces
Carbon [115]	Onion	Formation of carbon film on worn surfaces
Diamond [105]	–	Diamond nanoparticles act as a Polishing effect on friction specimen surfaces
Fe, Cu and Co [107]	Core–shell	Formation of metal nano-composite tribo-layer on friction surfaces
Serpentine/La(OH) <sub>3</sub> [108]	Granular	Formation of rare earth composite tribofilm on worn surfaces

**Table 7** (continued)

Nanoparticle [References]	Structure	Results of tribological effects/mechanisms on friction surfaces
Silver [124]	–	Formation of silver nano-tribofilm on worn surfaces
SiO <sub>2</sub> [121]	Nearly spherical	Rolling effect of SiO <sub>2</sub> nanoparticles on worn surfaces
Cu [99]	Spherical	Formation of Cu nano-protective layer on worn surfaces
Zinc aluminate (ZnAl <sub>2</sub> O <sub>4</sub> ) [109]	Spherical	ZnAl <sub>2</sub> O <sub>4</sub> nano-composite acts as a Nano-bearing and tribo-sintering effects on worn surfaces
Cu, Fe and Zn [114]	–	Formation of Cu, Fe and Zn metal tribofilm on worn surfaces
h-BN and graphene [110]	Both are 2D-nano-sheet	Tribo-sintering effect of H-BN/Graphene nano-structures on rubbed surfaces
Al <sub>2</sub> O <sub>3</sub> [112]	Spherical	Rolling effect of Al <sub>2</sub> O <sub>3</sub> nanoparticles on worn surfaces
Fly ash [90]	Uneven	Fly ash formed the protective film on frictional surfaces
rGO/GO [91]	Nanosheets	Patching effect of nanoparticles formed on worn surfaces
Halloysite clay [92]	Nanotube	Halloysite clay formed is a protective tribofilm on worn surfaces
Tiny CuO [93]	Spherical	Rolling effect promotes the copper oxide nanoparticle on worn surfaces
CNC [94]	Spherical	Formation of Cellulose Nano-Crystals on worn surfaces
DAG [95]	Nanosheets	Formation of graphene nano-tribofilm on worn surfaces
Al <sub>2</sub> O <sub>3</sub> and SiO <sub>2</sub> [96]	Spherical	Formation of Al <sub>2</sub> O <sub>3</sub> and SiO <sub>2</sub> nano-tribofilm on worn surfaces
Ni-MoS <sub>2</sub> [111]	Nanosheets	Formation of Ni-MoS <sub>2</sub> nano-tribofilm on worn surfaces
Graphite oxide extracted from waster carbon [98]	Nanosheets	Formation of thin-film on contacting surfaces

## Appendix 2

See Table 8.

**Table 8** Instruments used for tribological studies

Instruments used	References
Ball- on-disk friction and wear testing machine	[6, 10, 41, 47, 48, 55, 74, 86, 88, 89, 91, 95, 115, 120, 129]
Pin-on-disk friction and wear testing machine	[4, 7, 18, 19, 29, 34, 51, 54, 57, 79, 81, 87, 96, 102, 115, 121, 124, 126, 127, 130]
Tribology test rig (ASTM G181)	[8, 9]
Four ball tribological testing machine	[10, 12, 14, 18, 26, 27, 32, 33, 38, 40, 46, 52, 53, 56, 58, 60, 61, 72, 73, 78, 84, 85, 92, 98, 99, 104, 105, 107, 109–111, 114, 117, 118, 123, 125, 128, 131, 132]
Optimal SRV4 friction tester (ASTM D 5707)	[13, 20, 122]
Thrust ring friction and wear testing machine	[11, 12, 15, 126]
MMU-10G friction and wear testing machine	[15]
Rotation tribometer RT 4000	[129]
Disk-on-disk friction and wear testing machine	[24, 37, 106, 116, 129]
Reciprocating friction monitor	[17]
Rattling machine (shenzhou brand)	[21]
Block-on-ring	[22, 25, 26, 28, 31, 78, 105, 108, 113, 118]
High Frequency Reciprocating Rig (HFRR)	[24, 93, 112]
Ball-on-ring friction and wear testing machine	[31, 83]
Rotation disk tribometer	[49]
Engine friction test rig	[78]
Plint-TE77 reciprocating sliding friction tribo tester	[101]
MMU-5G friction and wear tester	[103]
Ring-on-ring tribo tester	[105]
MM-10W multifunctional friction tester	[94, 96, 108]
Ball-on-block MFT- R 4000 reciprocating friction and wear tester	[90]

### Appendix 3

See Table 9.

**Table 9** Summary of reported stability studies

References	Nanoparticle used	Base lubricant	Surfactant used	Stability testing method	Stability study
[5]	Cu–Zn	Vegetable oil, Paraffin oil and SAE oil	–	DLS and Zeta method	3 days (all three kind of nanolubricants)
[6]	WS <sub>2</sub>	PAO6	Oleylamine	Visual analysis	3 days
[8]	Al <sub>2</sub> O <sub>3</sub> , TiO <sub>2</sub> and Al <sub>2</sub> O <sub>3</sub> /TiO <sub>2</sub>	5W-30	OA	Visual analysis and UV spectroscopy	55 days
[9]	Al <sub>2</sub> O <sub>3</sub> and TiO <sub>2</sub>	5W-30	OA	UV spectroscopy and DLS	14 days
[11]	Al <sub>2</sub> O <sub>3</sub>	Lubricating oil	KH-560	Zeta potential	50 days
[12]	KH-560 surface-modified Al <sub>2</sub> O <sub>3</sub> /SiO <sub>2</sub>	Lubricating oil	–	Visual analysis	90 days
[14]	Al <sub>2</sub> O <sub>3</sub> –SiO <sub>2</sub>	PAG	–	Visual analysis, TEM and UV spectroscopy	30 days
[147]	TiO <sub>2</sub>	SAE 30 engine oil	OA	DLS and Zeta method	75 days
[126]	TiO <sub>2</sub>	Mineral oil	–	Visual analysis	Around 34 days
[16]	CuO	SAE20W50	–	Visual analysis	30 days
[30]	OA modified CuO	Liquid paraffin	–	Visual analysis	3 days
[36]	MWCNTs, G, CNBs and C <sub>60</sub>	SAE20W50	DDA	Visual analysis	30 days
[39]	Graphene nano-horns	PAG	–	DLS	14 days
[40]	Graphene	20W50	Polymeric ester	Zeta potential	0.01 mass% is stable
[72]	Graphene	Engine oil	–	Visual analysis	Above 30 days
[73]	Graphene	PAO10 & palm-oil tri-methylolpropane (TMP) ester	–	Visual analysis	20 days
[41]	Cu, TiO <sub>2</sub> and SWCNHs	Engine oil	–	DLS	14 days
[42]	MWCNTs	SAE20W50	DDA	Visual analysis	30 days
[45]	Graphite	Lubricating oil	CH-5	Visual analysis	About 1 ½ day
[50]	IF-MoS <sub>2</sub>	SAE-5W30	–	Visual analysis	365 days
[52]	MoS <sub>2</sub>	SAE 20W-40	Poly-isobutylene	DLS	10 days
[53]	MoS <sub>2</sub>	PAO	–	Zeta potential	MoS <sub>2</sub> nanosheets are maximum stable
[148]	Graphene	Glycerol	–	Visual analysis and centrifugal method	Excellent stability
[81]	Cu	Mineral oil and synthetic ester	–	Visual analysis	240 days
[84]	SiO <sub>2</sub>	Liquid paraffin	OA	Visual analysis	< 1 day
[84]	TiO <sub>2</sub> /SiO <sub>2</sub> , TiO <sub>2</sub>	Palm oil	–	Visual analysis and UV spectral analysis	3 days
[87]	CuO	Polyol ester	–	Visual analysis	< 1 day
[131]	Cu	SAE-30	Maleic anhydride (C <sub>4</sub> H <sub>2</sub> O <sub>3</sub> ), OA and Styrene (C <sub>8</sub> H <sub>8</sub> )	Visual analysis	21 days
[132]	ZnAl <sub>2</sub> O <sub>4</sub>	Lubricating oil	OA	Visual analysis and UV spectral analysis	Several days
[90]	Fly ash	PAO	OA	Visual analysis	7 days
[149]	Graphene	Glycerol	–	Visual analysis	Four months
[91]	rGO and GO	TMPTO and PAO40	–	Visual analysis, DLS and Refractometer	Great stability



**Table 9** (continued)

References	Nanoparticle used	Base lubricant	Surfactant used	Stability testing method	Stability study
[93]	Tiny CuO	PAO	–	Visual analysis and UV	Good dispersion
[94]	CNCs	SAE40	–	Visual analysis	Good suspension stability
[95]	DAG	Commercial lubricants	Dodecylamine	Visual analysis	8 days
[111]	Ni-MoS <sub>2</sub>	Commercial gear oil	–	Visual analysis, UV, Zeta potential	Excellent stability
[97]	Milled activated carbon	Solar glycol	Gum Arabic	Zeta potential, UV	Good stability

## References

- Heikkilä P. Bio-based carbon materials road-map. Espoo: VTT Technical Research Centre of Finland; 2016.
- Stachowiak G, Batchelor AW. Engineering Tribology [Internet]. Elsevier Science; 2013. Available from: <https://books.google.co.in/books?id=u69ptQAACAAJ>.
- Shahnazar S, Bagheri S, Abd Hamid SB. Enhancing lubricant properties by nanoparticle additives. *Int J Hydrogen Energy*. 2016;41:3153–70.
- Zhang W, Demydov D, Jahan MP, Mistry K, Erdemir A, Malshe AP. Fundamental understanding of the tribological and thermal behavior of Ag–MoS<sub>2</sub> nanoparticle-based multi-component lubricating system. *Wear*. 2012;288:9–16.
- Kumar MS, Vasu V, Gopal AV. Thermal conductivity and rheological studies for Cu–Zn hybrid nanofluids with various base fluids. *J Taiwan Inst Chem Eng*. 2016;66:321–7.
- Jiang Z, Zhang Y, Yang G, Gao C, Yu L, Zhang S, Zhang P. Synthesis of oil-soluble WS<sub>2</sub> nanosheets under mild condition and study of their effect on tribological properties of poly-alpha olefin under evaluated temperatures. *Tribol Int*. 2019;138:68–78.
- Chang H, Chen C-H, Tu H-S. The fabrication and effect of Bi and Bi/Cu nanoparticles on the tribological properties of SAE-30 lubricating oil. *J Comput Theor Nanosci*. 2015;12:852–7.
- Ahmed Ali MK, Xianjun H, Turkson RF, Peng Z, Chen X. Enhancing the thermophysical properties and tribological behaviour of engine oils using nano-lubricant additives. *RSC Adv*. 2016;6:77913–24.
- Ali MKA, Xianjun H, Mai L, Qingping C, Turkson RF, Bicheng C. Improving the tribological characteristics of piston ring assembly in automotive engines using Al<sub>2</sub>O<sub>3</sub> and TiO<sub>2</sub> nanomaterials as nano-lubricant additives. *Tribol Int*. 2016;103:540–54.
- Alves SM, Barros BS, Trajano MF, Ribeiro KSB, Moura E. Tribological behavior of vegetable oil-based lubricants with nanoparticles of oxides in boundary lubrication conditions. *Tribol Int*. 2013;65:28–36.
- Luo T, Wei X, Huang X, Huang L, Yang F. Tribological properties of Al<sub>2</sub>O<sub>3</sub> nanoparticles as lubricating oil additives. *Ceram Int*. 2014;40:7143–9.
- Jiao D, Zheng S, Wang Y, Guan R, Cao B. The tribology properties of alumina/silica composite nanoparticles as lubricant additives. *Appl Surf Sci*. 2011;257:5720–5.
- Pena-Paras L, Taha-Tijerina J, Garza L, Maldonado-Cortés D, Michalczewski R, Lapray C. Effect of CuO and Al<sub>2</sub>O<sub>3</sub> nanoparticle additives on the tribological behavior of fully formulated oils. *Wear*. 2015;332–333:1256–61.
- Zawawi NNM, Azmi WH, Redhwan AAM, Sharif MZ, Sharma KV. Thermo-physical properties of Al<sub>2</sub>O<sub>3</sub>–SiO<sub>2</sub>/PAG composite nanolubricant for refrigeration system. *Int J Refrig*. 2017;80:1–10.
- Luo T, Wei X, Zhao H, Cai G, Zheng X. Tribology properties of Al<sub>2</sub>O<sub>3</sub>/TiO<sub>2</sub> nanocomposites as lubricant additives. *Ceram Int*. 2014;40:10103–9.
- Farbod M, Kouhpeymaniasl R, Noghrehabadi AR. Morphology dependence of thermal and rheological properties of oil-based nanofluids of CuO nanostructures. *Colloids and Surf A Physicochem Eng Asp*. 2015;474:71–5.
- Nesappan S, Palanisamy N, Chandran M. Tribological Investigation of Copper (Cu) and Copper Oxide (CuO) Nanoparticles Based Nanolubricants for Machine Tool Slideways. Volume 2B: Advanced Manufacturing [Internet]. Montreal, Quebec, Canada: American Society of Mechanical Engineers; 2014 [cited 2019 Dec 17]. p. V02BT02A020. Available from: <https://asmcdigitalcollection.asme.org/IMECE/proceedings/IMECE2014/46445/Montreal,%20Quebec,%20Canada/254376>.
- Thottackkad MV, Perikinalil RK, Kumarapillai PN. Experimental evaluation on the tribological properties of coconut oil by the addition of CuO nanoparticles. *Int J Precis Eng Manuf*. 2012;13:111–6.
- Pisal AS, Chavan DS. Experimental investigation of tribological properties of engine oil with CuO nanoparticles. 2014;5.
- Zhang B, Xu Y, Gao F, Shi P, Xu B, Wu Y. Sliding friction and wear behaviors of surface-coated natural serpentine mineral powders as lubricant additive. *Appl Surf Sci*. 2011;257:2540–9.
- Li X, Zhao Y, Wu W, Chen J, Chu G, Zou H. Synthesis and characterizations of graphene–copper nanocomposites and their antifriction application. *J Ind Eng Chem*. 2014;20:2043–9.
- Hernández Battez A, Viesca JL, González R, Blanco D, Asedegbe E, Osorio A. Friction reduction properties of a CuO nanolubricant used as lubricant for a NiCrBSi coating. *Wear*. 2010;268:325–8.
- Hwang Y, Lee JK, Lee CH, Jung YM, Cheong SI, Lee CG, Ku BC, Jang SP. Stability and thermal conductivity characteristics of nanofluids. *Thermochim Acta*. 2007;455:70–4.
- Ghaednia H, Jackson RL, Khodadadi JM. Experimental analysis of stable CuO nanoparticle enhanced lubricants. *J Exp Nanosci*. 2015;10:1–18.
- Hernandez Battez A, Viesca Rodriguez JL, Gonzalez Rodriguez R, Fernandez Rico JE. Viscosity and Tribology of Copper Oxide Nanofluids. STLE/ASME 2008 International Joint Tribology Conference [Internet]. Miami, Florida, USA: ASME; 2008 [cited 2019 Dec 17]. p. 205–7. Available from: <http://proceedings.asmedigitalcollection.asme.org/proceeding.aspx?articleid=1630393>.
- Viesca JL, Hernandez Battez A, Gonzalez R, Chou R, Cabello JJ. Antiwear properties of carbon-coated copper nanoparticles used as an additive to a polyalphaolefin. *Tribol Int*. 2011;44:829–33.
- Hernandez Battez A, Fernandez Rico JE, Navas Arias A, Viesca Rodriguez JL, Chou Rodriguez R, Diaz Fernandez JM. The tribological behaviour of ZnO nanoparticles as an additive to PAO6. *Wear*. 2006;261:256–63.

28. Hernandez Battez A, Gonzalez R, Viesca JL, Fernandez JE, Diaz Fernandez JM, Machado A, Chou R, Riba J. CuO, ZrO<sub>2</sub> and ZnO nanoparticles as antiwear additive in oil lubricants. *Wear*. 2008;265:422–8.
29. Ingole S, Charanpahari A, Kakade A, Umare SS, Bhatt DV, Menghani J. Tribological behavior of nano TiO<sub>2</sub> as an additive in base oil. *Wear*. 2013;301:776–85.
30. Wan Q, Jin Y, Sun P, Ding Y. Tribological Behaviour of a Lubricant Oil Containing Boron Nitride Nanoparticles. *Procedia Engineering*. 2015;102:1038–45.
31. Peng DX, Kang Y, Hwang RM, Shyr SS, Chang YP. Tribological properties of diamond and SiO<sub>2</sub> nanoparticles added in paraffin. *Tribol Int*. 2009;42:911–7.
32. Xiang L, Gao C, Wang Y, Pan Z, Hu D. Tribological and tribochemical properties of magnetite nanoflakes as additives in oil lubricants. *Particuology*. 2014;17:136–44.
33. Li-jun W, Chu-wen G, Yamane R. Experimental research on tribological properties of Mn<sub>0.78</sub>Zn<sub>0.22</sub>Fe<sub>2</sub>O<sub>4</sub> magnetic fluids. *J Tribol*. 2008;130:031801.
34. Dinakaran R, Santhosh Kumar A, Selvakumar N, Jeyasubramanian K. Tribological behavior of nano ferrofluid in AISI 1005 steel. 2016; 2:10.
35. Hemmat Esfe M, Bahiraei M, Hajmohammad MH, Afrand M. Rheological characteristics of MgO/oil nanolubricants: experimental study and neural network modeling. *Int Commun Heat Mass Transf*. 2017;86:245–52.
36. Etefaghi E, Rashidi A, Ahmadi H, Mohtasebi SS, Pourkhalil M. Thermal and rheological properties of oil-based nanofluids from different carbon nanostructures. *Int Commun Heat Mass Transf*. 2013;48:178–82.
37. Lee K, Hwang Y, Cheong S, Kwon L, Kim S, Lee J. Performance evaluation of nano-lubricants of fullerene nanoparticles in refrigeration mineral oil. *Curr Appl Phys*. 2009;9:e128–31.
38. Ku B-C, Han Y-C, Lee J-E, Lee J-K, Park S-H, Hwang Y-J. Tribological effects of fullerene (C<sub>60</sub>) nanoparticles added in mineral lubricants according to its viscosity. *Int J Precis Eng Manuf*. 2010;11:607–11.
39. Zin V, Barison S, Agresti F, Colla L, Pagura C, Fabrizio M. Improved tribological and thermal properties of lubricants by graphene based nano-additive. 12.
40. Rasheed AK, Khalid M, Javeed A, Rashmi W, Gupta TCSM, Chan A. Heat transfer and tribological performance of graphene nanolubricant in an internal combustion engine. *Tribol Int*. 2016;103:504–15.
41. Zin V, Agresti F, Barison S, Colla L, Fabrizio M. Influence of Cu, TiO<sub>2</sub> nanoparticles and carbon nano-horns on tribological properties of engine oil. *J Nanosci Nanotechnol*. 2015;15:3590–8.
42. Etefaghi E, Ahmadi H, Rashidi A, Nouralishahi A, Mohtasebi SS. Preparation and thermal properties of oil-based nanofluid from multi-walled carbon nanotubes and engine oil as nanolubricant. *Int Commun Heat Mass Transf*. 2013;46:142–7.
43. Kaviyarasu T, Vasanthan B. Improvement of tribological and thermal properties of engine lubricant by using nano-materials. *J Chem Pharm Sci (JCHPS)*. 2015;7:208–11.
44. Peng Y, Xu Y, Geng J, Dearn KD, Hu X. Tribological assessment of coated piston ring-cylinder liner contacts under bio-oil lubricated conditions. *Tribol Int*. 2017;107:283–93.
45. Wang B, Wang X, Lou W, Hao J. Thermal conductivity and rheological properties of graphite/oil nanofluids. *Colloids Surf, A*. 2012;414:125–31.
46. Huang HD, Tu JP, Gan LP, Li CZ. An investigation on tribological properties of graphite nanosheets as oil additive. *Wear*. 2006;261:140–4.
47. Zhang Z, Cai Z, Peng J, Zhu M. Comparison of the tribology performance of nano-diesel soot and graphite particles as lubricant additives. *J Phys D Appl Phys*. 2016;49:045304.
48. Zhang Y, Tang H, Ji X, Li C, Chen L, Zhang D, Yang X, Zhang H. Synthesis of reduced graphene oxide/Cu nanoparticle composites and their tribological properties. *RSC Adv*. 2013;3:26086.
49. Yadgarov L, Petrone V, Rosentsveig R, Feldman Y, Tenne R, Senatore A. Tribological studies of rhenium doped fullerene-like MoS<sub>2</sub> nanoparticles in boundary, mixed and elasto-hydrodynamic lubrication conditions. *Wear*. 2013;297:1103–10.
50. Sgroi M, Gili F, Mangherini D, Lahouij I, Dassenoy F, Garcia I, Odriozola I, Kraft G. Friction reduction benefits in valvetrain system using IF-MoS<sub>2</sub> added engine oil. *Tribol Trans*. 2015;58:207–14.
51. Charoo MS, Wani MF. Tribological properties of h-BN nanoparticles as lubricant additive on cylinder liner and piston ring: tribological properties of h-BN nanoparticles as lubricant additive. *Lubr Sci*. 2017;29:241–54.
52. Srinivas V, Thakur RN, Jain AK. Antiwear, antifriction, and extreme pressure properties of motor bike engine oil dispersed with molybdenum disulfide nanoparticles. *Tribol Trans*. 2017;60:12–9.
53. Vattikuti SVP, Byon C. Synthesis and characterization of molybdenum disulfide nanoflowers and nanosheets: nanotribology. *J Nanomater*. 2015;2015:1–11.
54. Koshy CP, Rajendrakumar PK, Thottackkad MV. Evaluation of the tribological and thermo-physical properties of coconut oil added with MoS<sub>2</sub> nanoparticles at elevated temperatures. *Wear*. 2015;330–331:288–308.
55. Yi M, Zhang C. The synthesis of MoS<sub>2</sub> particles with different morphologies for tribological applications. *Tribol Int*. 2017;116:285–94.
56. Sunqing Q, Junxiu D, Guoxu C. Tribological properties of CeF<sub>3</sub> nanoparticles as additives in lubricating oils. *Wear*. 1999;230:35–8.
57. Thottackkad MV, Rajendrakumar PK, Prabhakaran NK. Tribological analysis of surfactant modified nanolubricants containing CeO<sub>2</sub> nanoparticles. *Tribol Mater Surf Interfaces*. 2014;8:125–30.
58. Liu R, Wei X, Tao D, Zhao Y. Study of preparation and tribological properties of rare earth nanoparticles in lubricating oil. *Tribol Int*. 2010;43:1082–6.
59. Yu L, Zhang L, Ye F, Sun M, Cheng X, Diao G. Preparation and tribological properties of surface-modified nano-Y<sub>2</sub>O<sub>3</sub> as additive in liquid paraffin. *Appl Surf Sci*. 2012;263:655–9.
60. Hu E, Hu X, Liu T, Song R, Dearn KD, Xu H. Effect of TiF<sub>3</sub> catalyst on the tribological properties of carbon black-contaminated engine oils. *Wear*. 2013;305:166–76.
61. Sunqing Q, Junxiu D, Guoxu C. Wear and friction behaviour of CaCO<sub>3</sub> nanoparticles used as additives in lubricating oils. *Lubr Sci*. 2000;12:205–12.
62. Paul G, Hirani H, Kuila T, Murmu NC. Nanolubricants dispersed with graphene and its derivatives: an assessment and review of the tribological performance. *Nanoscale*. 2019;11:3458–83.
63. Ali HM, Sajid MU, Arshad A. Heat Transfer Applications of TiO<sub>2</sub> Nanofluids. In: Janus M, editor. *Application of Titanium Dioxide* [Internet]. InTech; 2017 [cited 2020 Apr 20]. Available from <http://www.intechopen.com/books/application-of-titanium-dioxide/heat-transfer-applications-of-tiO2-nanofluids>.
64. Sajid MU, Ali HM, Sufyan A, Rashid D, Zahid SU, Rehman WU. Experimental investigation of TiO<sub>2</sub>-water nanofluid flow and heat transfer inside wavy mini-channel heat sinks. *J Therm Anal Calorim*. 2019;137:1279–94.
65. Soudagar MEM, Kalam MA, Sajid MU, Afzal A, Banapurmath NR, Akram N, Mane SD, Saleel CA. Thermal analyses of minichannels and use of mathematical and numerical models. *Numer Heat Transf Part A Appl*. 2020;77:497–537.
66. Babar H, Sajid M, Ali H. Viscosity of hybrid nanofluids: a critical review. *Therm Sci*. 2019;23:1713–54.

67. Wahab A, Hassan A, Qasim MA, Ali HM, Babar H, Sajid MU. Solar energy systems—potential of nanofluids. *J Mol Liq.* 2019;289:111049.
68. Sajid MU, Ali HM. Recent advances in application of nanofluids in heat transfer devices: a critical review. *Renew Sustain Energy Rev.* 2019;103:556–92.
69. Ali H, Babar H, Shah T, Sajid M, Qasim M, Javed S. Preparation techniques of TiO<sub>2</sub> nanofluids and challenges: a review. *Appl Sci.* 2018;8:587.
70. Yu W, Xie H. A review on nanofluids: preparation, stability mechanisms, and applications. *J Nanomater.* 2012;2012:1–17.
71. Sidik NAC, Mohammed HA, Alawi OA, Samion S. A review on preparation methods and challenges of nanofluids. *Int Commun Heat Mass Transf.* 2014;54:115–25.
72. Eswaraiyah V, Sankaranarayanan V, Ramaprabhu S. Graphene-based engine oil nanofluids for tribological applications. *ACS Appl Mater Interfaces.* 2011;3:4221–7.
73. Azman SSN, Zulkifli NWM, Masjuki H, Gulzar M, Zahid R. Study of tribological properties of lubricating oil blend added with graphene nanoplatelets. *J Mater Res.* 2016;31:1932–8.
74. Xu J, Tang H, Zhang K, Zhang H, Li C. Synthesis and tribological properties of flower-like MoS<sub>2</sub> nanostructures. 8.
75. Wu Y-Y, Kao M-J. Using TiO<sub>2</sub> nanofluid additive for engine lubrication oil. *Ind Lubr Tribol.* 2011;63:440–5.
76. Kong L, Sun J, Bao Y. Preparation, characterization and tribological mechanism of nanofluids. *RSC Adv.* 2017;7:12599–609.
77. Etefaghi E, Ahmadi H, Rashidi A, Mohtasebi S, Alaei M. Experimental evaluation of engine oil properties containing copper oxide nanoparticles as a nanoadditive. *Int J Ind Chem.* 2013;4:28.
78. Chou R, Battez AH, Cabello JJ, Viesca JL, Osorio A, Sagastume A. Tribological behavior of polyalphaolefin with the addition of nickel nanoparticles. *Tribol Int.* 2010;43:2327–32.
79. Jatti VS, Singh TP. Copper oxide nano-particles as friction-reduction and anti-wear additives in lubricating oil. *J Mech Sci Technol.* 2015;29:793–8.
80. Xie H, Jiang B, He J, Xia X, Pan F. Lubrication performance of MoS<sub>2</sub> and SiO<sub>2</sub> nanoparticles as lubricant additives in magnesium alloy–steel contacts. *Tribol Int.* 2016;93:63–70.
81. Guzman Borda FL, Ribeiro de Oliveira SJ, Seabra Monteiro Lazaro LM, KalabLeiroz AJ. Experimental investigation of the tribological behavior of lubricants with additive containing copper nanoparticles. *Tribol Int.* 2018;117:52–8.
82. Chen Y, Zhang Y, Zhang S, Yu L, Zhang P, Zhang Z. Preparation of nickel-based nanolubricants via a facile in situ one-step route and investigation of their tribological properties. *Tribol Lett.* 2013;51:73–83.
83. Peng D, Chen C, Kang Y, Chang Y, Chang S. Size effects of SiO<sub>2</sub> nanoparticles as oil additives on tribology of lubricant. *Ind Lubr Tribol.* 2010;62:111–20.
84. Gulzar M, Masjuki HH, Kalam MA, Varman M, Zulkifli NWM, Mufti RA, Zahid R, Yunus R. Dispersion stability and tribological characteristics of TiO<sub>2</sub>/SiO<sub>2</sub> nanocomposite-enriched bio-based lubricant. *Tribol Trans.* 2017;60:670–80.
85. Marko M, Kyle J, Branson B, Terrell E. Tribological improvements of dispersed nanodiamond additives in lubricating mineral oil. *J Tribol.* 2015;137:011802.
86. Kalin M, Kogovšek J, Remškar M. Mechanisms and improvements in the friction and wear behavior using MoS<sub>2</sub> nanotubes as potential oil additives. *Wear.* 2012;280–281:36–45.
87. Gobinath N, Ajmal M, Majilya S, Bharath K. Investigation of tribological characteristics of polyol ester–copper oxide nanolubricant. *Int J ChemTech Res.* 2017;10:93–7.
88. Guo M, Cai Z, Zhang Z, Zhu M. Characterization and lubrication performance of diesel soot nanoparticles as oil lubricant additives. *RSC Adv.* 2015;5:101965–74.
89. Reyes L, Loganathan A, Boesl B, Agarwal A. Effect of 2D boron nitride nanoplate additive on tribological properties of natural oils. *Tribol Lett.* 2016;64:41.
90. Cao Z, Xia Y. Study on the preparation and tribological properties of fly ash as lubricant additive for steel/steel pair. *Tribol Lett.* 2017;65:104.
91. Lineira del Rio JM, Lopez ER, Fernandez J, Garcia F. Tribological properties of dispersions based on reduced graphene oxide sheets and trimethylolpropane trioleate or PAO 40 oils. *J Mol Liq.* 2019;274:568–76.
92. Pena-Paras L, Maldonado-Cortes D, Garcia P, Irigoyen M, Taha-Tijerina J, Guerra J. Tribological performance of halloysite clay nanotubes as green lubricant additives. *Wear.* 2019;376–377:885–92.
93. Alves SM, Mello VS, Faria EA, Camargo APP. Nanolubricants developed from tiny CuO nanoparticles. *Tribol Int.* 2016;100:263–71.
94. Awang NW, Ramasamy D, Kadrigama K, Najafi G, Che Sidik NA. Study on friction and wear of Cellulose Nanocrystal (CNC) nanoparticle as lubricating additive in engine oil. *Int J Heat Mass Transf.* 2019;131:1196–204.
95. Paul G, Shit S, Hirani H, Kuila T, Murmu NC. Tribological behavior of dodecylamine functionalized graphene nanosheets dispersed engine oil nanolubricants. *Tribol Int.* 2019;131:605–19.
96. Kotia A, Ghosh GK, Srivastava I, Deval P, Ghosh SK. Mechanism for improvement of friction/wear by using Al<sub>2</sub>O<sub>3</sub> and SiO<sub>2</sub>/Gear oil nanolubricants. *J Alloys Compd.* 2019;782:592–9.
97. Poongavanam GK, Ramalingam V. Characteristics investigation on thermophysical properties of synthesized activated carbon nanoparticles dispersed in solar glycol. *Int J Therm Sci.* 2019;136:15–32.
98. Sivakumar B, Ranjan N, Ramaprabhu S, Kamaraj M. Tribological properties of graphite oxide derivative as nano-additive: synthesized from the waster carbon source. *Tribol Int.* 2020;142:105990.
99. Yang G, Chai S, Xiong X, Zhang S, Yu L, Zhang P. Preparation and tribological properties of surface modified Cu nanoparticles. *Trans Nonferrous Met Soc China.* 2012;22:366–72.
100. Dai W, Kheireddin B, Gao H, Liang H. Roles of nanoparticles in oil lubrication. *Tribol Int.* 2016;102:88–98.
101. Wu YY, Tsui WC, Liu TC. Experimental analysis of tribological properties of lubricating oils with nanoparticle additives. *Wear.* 2007;262:819–25.
102. Saurin N, Sanes J, Bermúdez M-D. New graphene/ionic liquid nanolubricants. *Mater Today Proc.* 2016;3:S227–32.
103. Qi X, Lu L, Jia Z, Yang Y, Liu H. Comparative tribological properties of magnesium hexasilicate and serpentine powder as lubricating oil additives under high temperature. *Tribol Int.* 2012;49:53–7.
104. Zhang Y, Xu Y, Yang Y, Zhang S, Zhang P, Zhang Z. Synthesis and tribological properties of oil-soluble copper nanoparticles as environmentally friendly lubricating oil additives. *Ind Lubr Tribol.* 2015;67:227–32.
105. Shenderova O, Vargas A, Turner S, Ivanov DM, Ivanov MG. Nanodiamond-based nanolubricants: investigation of friction surfaces. *Tribol Trans.* 2014;57:1051–7.
106. Choi Y, Lee C, Hwang Y, Park M, Lee J, Choi C, Jung M. Tribological behavior of copper nanoparticles as additives in oil. *Curr Appl Phys.* 2009;9:e124–7.
107. Padgurskas J, Rukuiza R, Prosycevas I, Kreivaitis R. Tribological properties of lubricant additives of Fe, Cu and Co nanoparticles. *Tribol Int.* 2013;60:224–32.
108. Zhao F, Bai Z, Fu Y, Zhao D, Yan C. Tribological properties of serpentine, La(OH)<sub>3</sub> and their composite particles as lubricant additives. *Wear.* 2012;288:72–7.

109. Song X, Zheng S, Zhang J, Li W, Chen Q, Cao B. Synthesis of monodispersed ZnAl<sub>2</sub>O<sub>4</sub> nanoparticles and their tribology properties as lubricant additives. *Mater Res Bull.* 2012;47:4305–10.
110. Taha-Tijerina J, Pena-Paras L, Narayanan TN, Garza L, Lapray C, Gonzalez J, Palacios E, Molina D, Garcia A, Maldonado D, Ajayan PM. Multifunctional nanofluids with 2D nanosheets for thermal and tribological management. *Wear.* 2013;302:1241–8.
111. Rajendhran N, Palanisamy S, Shyma AP, Venkatachalam R. Enhancing the thermophysical and tribological performance of gear oil using Ni-promoted ultrathin MoS<sub>2</sub> nanocomposites. *Tribol Int.* 2018;124:156–68.
112. Wu B, Song H, Li C, Song R, Zhang T, Hu X. Enhanced tribological properties of diesel engine oil with Nano-Lanthanum hydroxide/reduced graphene oxide composites. *Tribol Int.* 2020;141:105951.
113. Jeng Y-R, Huang Y-H, Tsai P-C, Hwang G-L. Tribological properties of carbon nanocapsule particles as lubricant additive. *J Tribol.* 2014;136:041801.
114. Asadauskas SJ, Kreivaitis R, Bikulčius G, Griguocienė A, Padgurskas J. Tribological effects of Cu, Fe and Zn nanoparticles, suspended in mineral and bio-based oils: tribological effects of suspended Cu, Fe and Zn nanoparticles. *Lubr Sci.* 2016;28:157–76.
115. Joly-Pottuz L, Vacher B, Ohmae N, Martin JM, Epicier T. Antiwear and friction reducing mechanisms of carbon nano-onions as lubricant additives. *Tribol Lett.* 2008;30:69–80.
116. Lee J, Cho S, Hwang Y, Lee C, Kim SH. Enhancement of lubrication properties of nano-oil by controlling the amount of fullerene nanoparticle additives. *Tribol Lett.* 2007;28:203–8.
117. Li Z, Hou X, Yu L, Zhang Z, Zhang P. Preparation of lanthanum trifluoride nanoparticles surface-capped by tributyl phosphate and evaluation of their tribological properties as lubricant additive in liquid paraffin. *Appl Surf Sci.* 2014;292:971–7.
118. Hu ZS, Lai R, Lou F, Wang LG, Chen ZL, Chen GX, Chen J, Dong X. Preparation and tribological properties of nanometer magnesium borate as lubricating oil additive. *Wear.* 2002;252:370–4.
119. Charoo MS, Wani MF. Friction and wear properties of nano-Si<sub>3</sub>N<sub>4</sub>/nano-SiC composite under nanolubricated conditions. *J Adv Ceram.* 2016;5:145–52.
120. Pan Q, Zhang X. Synthesis and tribological behavior of oil-soluble Cu nanoparticles as additive in SF15W/40 lubricating oil. *Rare Met Mater Eng.* 2010;39:1711–4.
121. Patil HH, Chavan DS, Pise AT. Tribological properties of SiO<sub>2</sub> nanoparticles added in SN-500 base oil. *Int J Eng Res.* 2013;2:6.
122. Zhang M, Wang X, Fu X, Xia Y. Performance and anti-wear mechanism of CaCO<sub>3</sub> nanoparticles as a green additive in poly-alpha-olefin. *Tribol Int.* 2009;42:1029–39.
123. Hu ZS, Dong JX, Chen GX, He JZ. Preparation and tribological properties of nanoparticle lanthanum borate. *Wear.* 2000;243:43–7.
124. Ghaednia H, Hossain MS, Jackson RL. Tribological performance of silver nanoparticle-enhanced polyethylene glycol lubricants. *Tribol Trans.* 2016;59:585–92.
125. Rashmi W, Khalid M, Lim, Xiao Y, Gupta, TCSM, Arwin, GZ. Tribological studies on graphene/TMP based nanolubricant [Internet]. 2017. Available from: <http://www.scopus.com/inward/record.url?scp=85011960957&partnerID=8YFLogXK>.
126. Krishna Sabareesh R, Gobinath N, Sajith V, Das S, Sobhan CB. Application of TiO<sub>2</sub> nanoparticles as a lubricant-additive for vapor compression refrigeration systems—an experimental investigation. *Int J Refrig.* 2012;35:1989–96.
127. Mohan N, Sharma M, Singh R, Kumar N. Tribological Properties of Automotive Lubricant SAE 20W-40 Containing Nano-Al<sub>2</sub>O<sub>3</sub> particles. 2014 [cited 2019 Dec 17]. p. 2014-01–2781. Available from <https://www.sae.org/content/2014-01-2781/>.
128. Qiu S, Zhou Z, Dong J, Chen G. Preparation of Ni nanoparticles and evaluation of their tribological performance as potential additives in oils. *J Tribol.* 2001;123:441–3.
129. Bogunovic L, Zuenkeler S, Toensing K, Anselmetti D. An oil-based lubrication system based on nanoparticulate TiO<sub>2</sub> with superior friction and wear properties. *Tribol Lett.* 2015;59:29.
130. Abate F, Senatore A, D'Agostino V, Leone C, Sarno M, Ciambelli P. Tribological properties of carbon nanotubes as lubricant additive. 2009; 3:4.
131. Gao D, Luo J. Synthesis of hyper-dispersant based on the application of nano-lubricants. *J Dispers Sci Technol.* 2016;37:1415–22.
132. Zulkifli NWM, Kalam MA, Masjuki HH, Yunus R. Experimental analysis of tribological properties of biolubricant with nanoparticle additive. *Procedia Eng.* 2013;68:152–7.
133. Dobrica MB, Fillon M. Mixed lubrication. In: Wang QJ, Chung Y-W, editors. *Encyclopedia of tribology*. Boston: Springer; 2013. p. 2284–91. [https://doi.org/10.1007/978-0-387-92897-5\\_27](https://doi.org/10.1007/978-0-387-92897-5_27).
134. Yan Y. Tribology and tribo-corrosion testing and analysis of metallic biomaterials. *Metals for Biomedical Devices [Internet]. Elsevier;* 2010 [cited 2019 Dec 17]. p. 178–201. Available from: <https://linkinghub.elsevier.com/retrieve/pii/B9781845694340500073>.
135. Aldred EM, Buck C, Vall K. Chapter 3: Bonds found in biological chemistry. In: Aldred EM, Buck C, Vall K, editors. *Pharmacology*. Edinburgh: Churchill Livingstone; 2009. p. 11–9.
136. Feher J. Chemical foundations of physiology I. 2012. p. 32–42.
137. Prasher R, Bhattacharya P, Phelan PE. Thermal conductivity of nanoscale colloidal solutions (nanofluids). *Phys Rev Lett.* 2005;94:025901.
138. Wang X-Q, Mujumdar AS. Heat transfer characteristics of nanofluids: a review. *Int J Therm Sci.* 2007;46:1–19.
139. Jang SP, Choi SUS. Role of Brownian motion in the enhanced thermal conductivity of nanofluids. *Appl Phys Lett.* 2004;84:4316–8.
140. Kole M, Dey TK. Role of interfacial layer and clustering on the effective thermal conductivity of CuO–gear oil nanofluids. *Exp Thermal Fluid Sci.* 2011;35:1490–5.
141. Kole M, Dey TK. Enhanced thermophysical properties of copper nanoparticles dispersed in gear oil. *Appl Therm Eng.* 2013;56:45–53.
142. Prasher R, Phelan PE, Bhattacharya P. Effect of aggregation kinetics on the thermal conductivity of nanoscale colloidal solutions (nanofluid). *Nano Lett.* 2006;6:1529–34.
143. Wang W, Li P, Sheng S, Tian H, Zhang H, Zhang X. Influence of hydrocarbon base oil molecular structure on lubricating properties in nano-scale thin film. *Tribol Lett.* 2019;67:111.
144. Dhinesh Kumar D, Valan AA. A comprehensive review of preparation, characterization, properties and stability of hybrid nanofluids. *Renew Sustain Energy Rev.* 2018;81:1669–89.
145. Khan AI, Valan AA. A review of influence of nanoparticle synthesis and geometrical parameters on thermophysical properties and stability of nanofluids. *Therm Sci Eng Progr.* 2019;11:334–64.
146. Babar H, Ali HM. Towards hybrid nanofluids: preparation, thermophysical properties, applications, and challenges. *J Mol Liq.* 2019;281:598–633.
147. Binu KG, Shenoy BS, Rao DS, Pai R. Static characteristics of a fluid film bearing with TiO<sub>2</sub> based nanolubricant using the modified Krieger–Dougherty viscosity model and couple stress model. *Tribol Int.* 2014;75:69–79.
148. Shaharuddin NA, Walvekar RG, Shahbaz K. Stability studies of graphene nanolubricants using ionic liquid analogues. :2.
149. Moghaddam MB, Goharshadi EK, Entezari MH, Nancarrow P. Preparation, characterization, and rheological properties of graphene–glycerol nanofluids. *Chem Eng J.* 2013;231:365–72.

150. Ghadimi A, Saidur R, Metselaar HSC. A review of nanofluid stability properties and characterization in stationary conditions. *Int J Heat Mass Transf.* 2011;54:4051–68.
151. Sajid MU, Ali HM. Thermal conductivity of hybrid nanofluids: a critical review. *Int J Heat Mass Transf.* 2018;126:211–34.
152. Yu F, Chen Y, Liang X, Xu J, Lee C, Liang Q, Tao P, Deng T. Dispersion stability of thermal nanofluids. *Progr Nat Sci Mater Int.* 2017;27:531–42.
153. Hwang Y, Park HS, Lee JK, Jung WH. Thermal conductivity and lubrication characteristics of nanofluids. *Curr Appl Phys.* 2006;6:e67–71.

**Publisher's Note** Springer Nature remains neutral with regard to jurisdictional claims in published maps and institutional affiliations.